sustainability

IMPACT FACTOR 4.1

CITESCORE 8.9

Article

Sustainable Stabilization of Kaolin Clay Using Lime and Ignimbritic Volcanic Tuff Waste: Mechanical and Microstructural Performance

Burak Dereli, Halil İbrahim Günaydın and Ömür Çimen

Special Issue
Sustainable Materials, Waste Management, and Recycling

Edited by
Dr. Kiadtisak Saenboonruang and Dr. Worawat Poltabtim

MDPI

https://doi.org/10.3390/su18136438

sustainability

MDPI

Article

Sustainable Stabilization of Kaolin Clay Using Lime and Ignimbritic Volcanic Tuff Waste: Mechanical and Microstructural Performance

Burak Dereli [1], Halil İbrahim Günaydın [2,*] and Ömür Çimen [3]

[1] Construction Department, Tatvan Vocational School, Bitlis Eren University, Bitlis 13200, Türkiye; bdereli@beu.edu.tr
[2] Construction Department, Vocational School of Technical Sciences, Akdeniz University, Antalya 07060, Türkiye
[3] Department of Civil Engineering, Faculty of Engineering and Natural Sciences, Süleyman Demirel University, Isparta 32260, Türkiye; omurcimen@sdu.edu.tr
* Correspondence: hgunaydin@akdeniz.edu.tr

Abstract

Lime-based stabilization of clayey soils remains a cornerstone of ground improvement, yet the high carbon footprint of lime production drives the search for sustainable supplementary binders derived from industrial and quarrying wastes. Volcanic tuff waste (VTW), a fine powder by-product of wet cutting of ignimbritic tuff blocks, is an underutilized quarrying residue, already fine enough to use directly without grinding or thermal processing, yet its use as a supplementary binder in lime-stabilized clays has not been systematically investigated. This study evaluates VTW sourced from Ahlat (Bitlis, Türkiye) in kaolin clay stabilized with 6% lime, with VTW added at 0%, 10%, 15%, and 20% by dry weight. Mixtures were characterized through Atterberg limits, compaction, unconfined compressive strength (UCS) at 1–28 days, California Bearing Ratio (CBR), XRD, SEM, and FTIR. VTW reduced plasticity index, increased maximum dry density, and lowered optimum moisture content. The 15% VTW mixture achieved the highest 28-day UCS of 4296 kPa, a 17.2% improvement over the lime-only control, and the highest CBR of 80%. XRD revealed Tobermorite 9 Å formation, while SEM and FTIR confirmed cementitious gel phases consistent with pozzolanic reactions. The findings demonstrate that ignimbritic VTW, used directly without processing, is an effective supplementary binder that partially replaces carbon-intensive lime, supporting low-carbon, cost-effective stabilization and the valorization of quarrying waste within a circular economy framework.

Keywords: volcanic tuff waste; ignimbrite; lime stabilization; kaolin clay; pozzolanic reaction; waste valorization; circular economy; sustainable ground improvement; low-carbon stabilization; unconfined compressive strength

Check for updates

Academic Editors: Kiadtisak Saenboonruang and Worawat Poltabtim

Received: 13 May 2026
Revised: 13 June 2026
Accepted: 15 June 2026
Published: 24 June 2026

Copyright: © 2026 by the authors. Licensee MDPI, Basel, Switzerland. This article is an open access article distributed under the terms and conditions of the Creative Commons Attribution (CC BY) license.

1. Introduction

Clayey soils are inherently prone to unfavourable engineering behaviour owing to their fine particle size, high specific surface area, surface activity, and strong affinity for water, all of which significantly influence their mechanical response [1]. These soils commonly exhibit low strength, high compressibility, and pronounced volume change behaviour, including swelling and shrinkage, resulting in reduced bearing capacity and poor performance of geotechnical structures such as road subgrades, embankments, and

shallow foundations [2,3]. Consequently, excessive settlement, cracking, and instability frequently occur, making the stabilization of clayey soils a critical necessity in geotechnical engineering practice [4,5]. However, conventional stabilization practices rely heavily on energy-intensive binders such as lime and cement, whose production accounts for approximately 7–8% of global anthropogenic CO_2 emissions [6–9], creating a pressing need for more sustainable stabilization strategies.

Despite these environmental concerns, lime remains one of the most widely adopted binders for the chemical stabilization of clayey soils, owing to its proven effectiveness in modifying soil behaviour and promoting long-term strength development [10–14]. The addition of lime initially triggers rapid reactions such as cation exchange and flocculation–agglomeration [15], which modify the soil microstructure, reduce plasticity, and improve workability [16,17]. With time, pozzolanic reactions occur between calcium supplied by lime and the silica and alumina derived from the clay minerals [18,19], resulting in the formation of cementitious hydration products, primarily calcium silicate hydrate (C–S–H) and calcium aluminate hydrate (C–A–H) [20–22]. These hydration products are mainly responsible for the enhanced strength, stiffness, and durability of the stabilized soil [23–26].

Although lime stabilization is a well-established and effective approach for improving the engineering properties of clayey soils, extensive research has shown that the incorporation of supplementary pozzolanic materials alongside lime can lead to significant improvements in strength compared to lime stabilization alone [27–29]. This enhancement is primarily attributed to the additional cementitious products formed through the reaction between calcium hydroxide released by lime and the reactive silica and alumina supplied by the pozzolanic additive, thereby enhancing the overall stabilization performance [30]. In parallel, the economic and environmental burdens associated with lime production, including high energy consumption and significant carbon dioxide emissions, have prompted increasing interest in hybrid stabilization approaches in which lime is partially complemented by industrial by-products or natural pozzolans [7,31]. Such approaches not only aim to improve engineering performance but also support more sustainable material use by utilizing waste or naturally available resources. These dual motivations—performance enhancement and environmental responsibility—have shaped the direction of research on lime-based hybrid stabilization systems over the past two decades.

Within this framework, industrial and agricultural by-products have been among the most widely investigated supplementary binders, with materials such as fly ash (FA), ground granulated blast furnace slag (GGBS), silica fume (SF), and rice husk ash (RHA) attracting particular attention. Numerous studies have reported significant improvements in unconfined compressive strength (UCS), plasticity properties, and long-term performance when these materials are combined with lime [32–36]. The effectiveness of these additives is largely governed by their reactive silica and alumina content, which participate in pozzolanic reactions with calcium hydroxide to form additional cementitious products, thereby enhancing the stabilization provided by lime alone [37]. However, these widely used industrial by-products are increasingly recognized as resource-constrained materials, with global supplies that are finite, already close to fully utilized, and in several regions declining as coal-fired power and primary steelmaking are phased out [38–40]. Building on these findings, attention has progressively shifted toward natural pozzolanic materials, which offer comparable reactivity while presenting advantages in terms of regional availability and reduced processing requirements [41,42]. Among these, volcanic-origin materials are particularly noteworthy owing to their high silica and alumina contents and partially amorphous structure, which enhances their reactivity under the high-pH conditions generated by lime hydration [43].

Within the broader category of volcanic-origin pozzolanic materials, research interest has been predominantly directed toward materials such as volcanic ash, zeolite, and pumice, all of which have been extensively investigated as supplementary materials in lime-stabilized soils [44–50]. These materials, however, differ from ignimbritic tuff in both origin and structure: zeolites typically form through the alteration of the glassy phase of volcanic tuff, while pumice represents porous volcanic glass fragments that may occur within it, so that ignimbritic tuff constitutes the parent rock from which such materials derive rather than an altered or fragmentary product [43,51]. Compositionally, ignimbritic materials are distinguished less by any single oxide ratio than by their glass-rich, multi-phase character, in which a reactive amorphous phase coexists with a complex feldspar-, silica-, and oxide-bearing mineral assemblage [52]. It is this reactive amorphous fraction—rather than a particular bulk oxide content—that primarily governs the pozzolanic behaviour of such materials under the alkaline conditions generated by lime. Volcanic tuffs, formed from consolidated pyroclastic deposits, have also attracted some research attention; however, their use in this context has been largely confined to geopolymer production and building material applications [53–55], while their potential as a supplementary material in lime-based soil stabilization remains largely unexplored. Studies involving pyroclastic soils stabilized with lime have demonstrated the occurrence of pozzolanic reactions and associated microstructural modifications [51,56], yet these investigations focused on pyroclastic soils as the host material rather than on ignimbritic tuff as a supplementary stabilizing agent. The waste generated during the cutting and processing of this ignimbritic tuff—hereafter referred to as volcanic tuff waste (VTW)—is a fine powder by-product that retains the pozzolanic characteristics of the parent material while constituting an underutilized quarrying waste stream. In contrast to most supplementary pozzolans studied in lime-based stabilization—including natural volcanic pozzolans, which often require crushing or grinding to reach a reactive fineness, as well as industrial pozzolans such as fly ash, GGBS, and silica fume—VTW arises directly from the wet-cutting process already in a fine powder form. Volcanic quarrying and stone processing generate large volumes of fine residue that are typically stockpiled or landfilled [57], and comparable volcanic quarry by-products have recently been shown to perform effectively as low-carbon alternatives to fly ash [58]. It can therefore be valorized in its as-received state, without any additional grinding or thermal processing, combining the resource benefit of a waste-derived material with the practical advantage of requiring no fineness preparation. Despite these advantages, the use of ignimbritic VTW as a supplementary material in lime-based stabilization of clayey soils has not, to the best of the authors' knowledge, been systematically investigated. The VTW used in this study originates from ignimbritic deposits associated with the Nemrut volcanic system in the Ahlat district of Bitlis Province, eastern Türkiye, a source that has been characterized in previous studies [52,59,60].

In light of the identified research gap, this study aims to evaluate the stabilization potential of VTW as a supplementary binder in lime-stabilized kaolin clay. Kaolin was selected as a model clay to minimize mineralogical variability and isolate the pozzolanic contribution of VTW under controlled conditions, providing a reproducible baseline against which future studies on natural problematic clays can be benchmarked. A constant lime content of 6% was adopted, while VTW was incorporated at proportions of 0%, 10%, 15%, and 20% by total dry weight. The engineering behaviour of the mixtures was evaluated through Atterberg limits, standard compaction, unconfined compressive strength (UCS) at curing periods of 1, 7, 14, 21, and 28 days, and California Bearing Ratio (CBR) tests. To elucidate the governing stabilization mechanisms, X-ray diffraction (XRD), scanning electron microscopy (SEM), and Fourier-transform infrared spectroscopy (FTIR) analyses were performed on selected samples. This study contributes to the growing body of

research on pozzolanic materials by providing insight into the pozzolanic reactivity of ignimbritic VTW in lime-based systems and demonstrating its viability as a supplementary binder for clayey soil stabilization. Importantly, because VTW is used directly in its as-received waste form, the approach avoids energy-intensive processing and partially replaces lime—a major source of CO_2 emissions in conventional stabilization—thereby reducing both the environmental footprint and the cost of treatment. In this way, the findings support the valorization of an underutilized quarrying waste and offer a sustainable, circular-economy-oriented alternative to conventional pozzolanic additives.

2. Materials and Methods

2.1. Materials

2.1.1. Soil

The soil used in this study was a commercially sourced kaolin clay, provided by Utelka (Balıkesir, Türkiye). The physical properties of the soil are detailed in Table 1. The liquid limit (LL), plastic limit (PL), and plasticity index (PI) were determined to be 32.5%, 21.7%, and 10.7%, respectively. According to the Unified Soil Classification System (USCS), the soil was classified as low-plasticity clay (CL). The chemical composition was determined by wavelength-dispersive X-ray fluorescence (WDXRF) spectrometry (Rigaku ZSX Primus II, Rigaku Corporation, Tokyo, Japan) on pressed powder pellets, and the results are presented in Table 2.

Table 1. Physical and compaction properties of the kaolin clay used in this study.

Parameter	Standard	Value
Specific gravity (Gs)	ASTM D854-14 [61]	2.62
Liquid limit (LL, %)	ASTM D4318-17 [62]	32.50
Plastic limit (PL, %)	ASTM D4318-17 [62]	21.70
Plasticity index (PI, %)	ASTM D4318-17 [62]	10.70
Soil classification (USCS)	ASTM D2487-17 [63]	CL
Maximum dry density (MDD, kN/m^3)	ASTM D698-12 [64]	16.39
Optimum moisture content (OMC, %)	ASTM D698-12 [64]	18.60

Table 2. Chemical composition of kaolin, VTW, and lime determined by XRF analysis (wt.%).

Compound	Kaolin	Volcanic Tuff Waste	Lime
SiO_2	76.41	69.78	–
Al_2O_3	19.09	10.56	–
Fe_2O_3	1.52	6.70	–
CaO	0.81	1.76	–
MgO	–	0.10	–
SO_3	1.02	<0.0013	–
K_2O	0.39	5.46	–
Na_2O	–	4.43	–
Cr_2O_3	–	–	–
Mn_2O_3	–	0.15	–
P_2O_5	0.67	–	–
$CaCO_3$	–	–	1.10
$MgSO_4$	–	–	1.80
$Ca(OH)_2$	–	–	97.10
Total	99.93	98.96	100.00

2.1.2. Volcanic Tuff Waste

Volcanic tuff waste (VTW) was obtained from a local stone processing facility operating in the Ahlat district of Bitlis Province, eastern Türkiye, where ignimbritic tuff blocks are cut for use as building stones. The VTW is a fine powder by-product of the wet cutting process and originates from ignimbritic deposits associated with the volcanic activity of the Nemrut volcanic system; the characteristics of volcanic tuffs from the Ahlat region have been well documented in previous studies [52,59,60]. Upon receipt, the as-received powder was dry-sieved through a 74 µm (No. 200) sieve, with the entire material passing through; the sieved fraction was used without any further grinding or thermal processing. The physical and pozzolanic properties of the VTW used in this study are summarized in Table 3.

Table 3. Physical and pozzolanic properties of VTW.

Property	Method	Value
Specific gravity (Gs)	ASTM D854-14	2.52
Material passing 74 µm (No. 200) sieve (%)	Dry sieving	100
Material passing 45 µm (No. 325) sieve (%)	Dry sieving	98.1
Blaine fineness (cm^2/g)	ASTM C204 [65]	2380
$SiO_2 + Al_2O_3 + Fe_2O_3$ (wt.%)	XRF	87.04
SO_3 (wt.%)	XRF	<0.0013
Pozzolanic activity, 7-day comp. strength of lime–pozzolan mortar (MPa)	TS 25 [66]	4.40

The chemical composition of VTW, determined by XRF analysis (Rigaku ZSX Primus II), is presented in Table 2 and reveals a dominance of SiO_2 and Al_2O_3, with Fe_2O_3, CaO, MgO, and alkali oxides occurring in minor proportions. This oxide distribution is consistent with compositions reported for ignimbritic materials from the Ahlat region [67]. The combined content of $SiO_2 + Al_2O_3 + Fe_2O_3$ reaches 87.04%, with a very low SO_3 content (<0.0013%), an oxide distribution characteristic of reactive natural pozzolans and indicative of a chemically stable, low-sulfate material. The fine particle size of the VTW, reflected in its complete passing through the 75 µm sieve and a Blaine fineness of 2380 cm^2/g, provides a large reactive surface area favourable for pozzolanic interaction with lime. The pozzolanic reactivity of VTW was assessed through the 7-day compressive strength of a lime–pozzolan mortar, determined according to the TS 25 procedure, which reached 4.40 MPa (Table 3). This result is consistent with the study by Toprak et al. [53], which classified Ahlat Stone from the same source region as a natural pozzolan based on the ASTM C311/C311M strength activity index test [68], supporting the suitability of VTW as a supplementary binder in lime-based stabilization systems.

2.1.3. Lime

Hydrated lime (calcium hydroxide, $Ca(OH)_2$) supplied by Kimyalab (İstanbul, Türkiye) was used as the chemical stabilizing agent. The product had a $Ca(OH)_2$ content of 97.10%, with minor amounts of $CaCO_3$ (1.10%) and $MgSO_4$ (1.80%) (Table 2), also determined by WDXRF analysis (Rigaku ZSX Primus II).

2.2. pH-Based Assessment of Lime Content

The initial consumption of lime (ICL) for the kaolin clay was determined using the Eades and Grim pH test (ASTM D6276-19) [69,70]. The results indicated that the ICL threshold, defined by a pH value of 12.4, was reached at 4% lime content, as illustrated in Figure 1. However, recent studies suggest that while ICL dosages effectively improve soil workability and modification [71], they often fail to provide the necessary calcium reserve

for long-term mechanical performance [72,73]. Specifically, Babanas and Courcelles [74] recommend increasing the dosage by 0.5% to 1.0% above the ICL to ensure maximum compressive strength. Furthermore, investigations on similar kaolinitic and expansive soils have reported that dosages in the 4–6% or even 6–8% range are essential for significant bearing capacity enhancement and sustained pozzolanic activity [34,75,76]. This consideration is particularly relevant for the lime–VTW system of the present study. Whereas the 4% ICL dosage is sufficient to raise the pore-fluid pH and satisfy the initial cation-exchange and modification demand of the kaolinite, lime added above the ICL becomes available for the pozzolanic reaction, in which the reactive silica and alumina supplied by VTW progressively consume calcium hydroxide to form C–S–H/C–A–S–H over the curing period [77]. Because this pozzolanic reaction proceeds only as long as free calcium remains available [78], a dosage fixed at the ICL would be largely depleted by the clay modification reactions, leaving insufficient calcium reserve to sustain the additional pozzolanic demand introduced by VTW [79]. Consequently, a constant lime content of 6%—approximately 2% above the ICL—was selected to maintain calcium availability for the lime–VTW pozzolanic reaction and to ensure adequate conditions for long-term structural stabilization. Consequently, a constant lime content of 6%—approximately 2% above the ICL—was selected to maintain calcium availability for the lime–VTW pozzolanic reaction and to ensure adequate conditions for long-term structural stabilization.

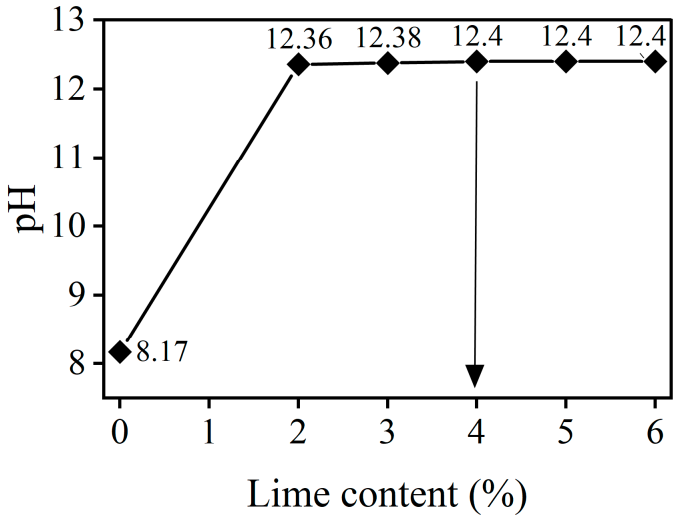


Figure 1. Variation in pH with lime content for kaolin clay.

2.3. Mixture Design

In this study, a series of kaolin clay mixtures stabilized with lime and VTW were prepared to conduct physical, mechanical, and microstructural characterization tests, including consistency limit, standard compaction, CBR, UCS, XRD, FTIR, and SEM analyses. The mixture proportions are summarized in Table 4. The mixtures were prepared in two series: the lime-free series, in which kaolin was partially substituted with VTW at proportions of 0%, 10%, 15%, and 20% by total dry weight without any lime addition; and the 6% lime series, in which the same VTW substitution proportions were prepared with the addition of a constant 6% lime content by total dry weight. All percentages refer to the proportion of each component in the final dry mixture, with the total dry mass of each mixture normalized to 100%. Atterberg, compaction, CBR, and UCS tests were performed on all eight mixtures, whereas XRD, FTIR, and SEM analyses were carried out on selected representative samples (see Section 2.4.5).

Table 4. Mixture proportions of the studied kaolin–VTW–lime mixtures.

Mixture Series	Kaolin (%)	VTW (%)	Lime (%)
Lime-free series	100	0	0
	90	10	0
	85	15	0
	80	20	0
6% lime series	94	0	6
	84	10	6
	79	15	6
	74	20	6

2.4. Experimental Program and Testing Methods

2.4.1. Atterberg Limits

Atterberg limit tests were conducted to evaluate the effects of VTW and lime additions on the consistency characteristics of the kaolin mixtures. The liquid limit (LL) and plastic limit (PL) tests were performed in accordance with ASTM D4318-17 [62] on all eight mixtures, including both the lime-free and 6% lime series. For each mixture, three replicate tests were performed, and the reported values represent the mean of the three replicates. The plasticity index (PI) was subsequently calculated as the difference between the mean LL and PL values.

2.4.2. Standard Compaction Test

Standard Proctor compaction tests were performed to determine the compaction characteristics of the kaolin mixtures and to assess the influence of VTW and lime additions on the MDD and OMC. The tests were conducted in accordance with ASTM D698-12 [64] on all eight mixtures. For each mixture, three replicate tests were performed, and the reported MDD and OMC values represent the mean of the three replicates.

2.4.3. Unconfined Compressive Strength (UCS) Test

The UCS tests were conducted to evaluate the mechanical behaviour of the soil mixtures. Cylindrical specimens with dimensions of 50 mm in diameter and 100 mm in height were prepared for testing. For each mixture, the required amount of material was mixed with water at its corresponding OMC until a homogeneous consistency was achieved. These mixtures were then statically compacted in three equal layers into cylindrical split moulds using a hydraulic compaction device to achieve the target MDD previously determined from the standard Proctor compaction tests. After compaction, the specimens were immediately extruded from the moulds and sealed with an impermeable polymer film to prevent moisture loss during curing. The wrapped specimens were then placed in a controlled curing chamber maintained at a constant temperature of 25 $\pm$ 1 °C and a relative humidity of approximately 99%. Lime-free specimens were cured for 1 day, while 6% lime-stabilized mixtures were cured for 1, 7, 14, 21, and 28 days; all specimens were maintained under the same controlled curing conditions described above.

The UCS tests were performed in accordance with ASTM D2166/D2166M [80] using a triaxial compression apparatus operated under unconfined conditions. The loading system was equipped with a 10 kN load cell, and a constant axial displacement rate of 1.1 mm/min was applied during the tests. For each VTW content–curing time combination, three identical specimens were tested, and the reported UCS values correspond to the mean of these replicates, with the associated standard deviations presented as error bars in the figures. This approach was consistently applied to both the lime-free and 6% lime-stabilized series.

2.4.4. California Bearing Ratio (CBR) Test

The CBR tests were performed in accordance with ASTM D1883-21 [81] to evaluate the bearing capacity and swell behaviour of the kaolin mixtures under soaked conditions. These tests were carried out on all eight mixtures, including both the lime-free and 6% lime series. Specimens were prepared in standard CBR moulds (152.4 mm in diameter and 177.8 mm in height) equipped with a 50 mm collar and a base plate. A 150.8 mm diameter and 61.4 mm high spacer disc was placed at the base of each mould prior to compaction. Mixtures were compacted at their corresponding OMC and target MDD using the standard Proctor energy in three equal layers.

Following compaction, the specimens were soaked in water for 96 h (4 days) to achieve full saturation. During this period, the swelling deformation was monitored using a dial gauge mounted on the perforated swell plate. The CBR swell value was calculated as the percentage change in specimen height relative to the initial height after the soaking period. After soaking, the specimens were drained for 15 min and then subjected to penetration testing using a piston with a diameter of 49.6 mm at a constant penetration rate of 1.27 mm/min. The CBR value was determined as the ratio of the measured penetration resistance at 2.54 mm penetration depth to the standard penetration resistance, expressed as a percentage.

For each mixture, three replicate tests were performed, and the reported CBR and CBR swell values represent the mean of the three replicates.

2.4.5. Mineralogical and Microstructural Characterization

Mineralogical and microstructural analyses were performed using XRD, FTIR, and SEM techniques on selected representative samples to investigate the transformations associated with VTW addition and lime stabilization. The samples included pure kaolin, pure VTW, the lime-stabilized kaolin without VTW (kaolin + 6% lime), and the optimum mixture (kaolin + 15% VTW + 6% lime), which exhibited the highest 28-day UCS (see Section 3.3). The specific samples used for each analysis are detailed in the corresponding result sections. Sub-samples were obtained from cured specimens after the 28-day curing period.

The XRD analyses were performed using a Bruker D8 Advance Twin-Twin X-ray diffractometer (Bruker AXS GmbH, Karlsruhe, Germany) equipped with Cu-Kα radiation (λ = 1.5406 Å). Diffraction patterns were recorded at room temperature over a 2θ range of 5–85°, with a step size of 0.05° and a scan rate of 0.1 s/step. The X-ray tube was operated at 40 kV and 30 mA.

FTIR analyses were conducted to identify functional groups and bonding characteristics within the samples. The spectra were obtained in the mid-infrared region using a JASCO FT/IR 4700 spectrometer (JASCO Corporation, Tokyo, Japan) operating in attenuated total reflectance (ATR) mode with a diamond ATR accessory. The measurements were carried out with a resolution of 4 cm^{-1}, and 32 accumulated scans per sample over the spectral range of 4000–400 cm^{-1} at room temperature.

The microstructural features and surface morphology of the samples were examined using a field emission gun scanning electron microscope (FEG-SEM, FEI Quanta FEG 250, FEI Company, Hillsboro, OR, USA). Prior to imaging, the samples were coated with a thin carbon layer to enhance electrical conductivity. SEM observations were carried out under low-vacuum conditions using secondary electron (SE) and backscattered electron (BSE) detectors. Micrographs were acquired at various magnifications, and representative images at a magnification of 20,000× are presented in this study.

A schematic overview of the experimental program, including the materials used, sample preparation procedure, and testing sequence, is presented in Figure 2.

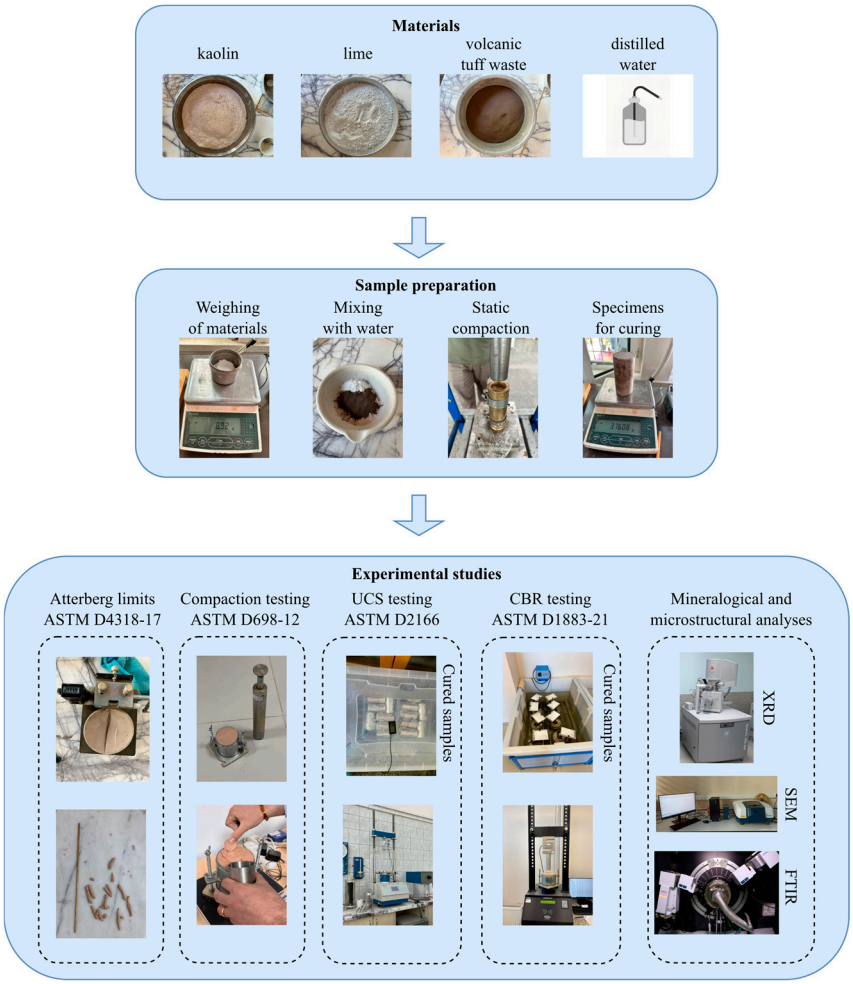


Figure 2. Schematic representation of the experimental program followed in this study, including the materials used, sample preparation procedure, and the experimental studies performed on the kaolin–VTW–lime mixtures.

2.5. Statistical Analysis

Statistical analysis was performed to interpret the relationships among the measured geotechnical parameters. Pearson correlation analysis was conducted using OriginPro 2026 (OriginLab Corporation, Northampton, MA, USA) to quantify the strength and direction of the linear associations between variables, and two-tailed significance (p-values) was determined for each correlation. The analysis included VTW content, lime content, curing period, index properties (LL, PL, PI), compaction parameters (MDD, OMC), and mechanical properties (UCS, CBR, CBR swell). For each mixture, the mean of three replicates was used. Because the lime-free specimens were tested for UCS only at 1 day, no values were imputed or extrapolated for the unmeasured curing periods of this series; the analysis was therefore carried out on an observed-case (long-format) dataset, comprising $n = 4$ observations for the lime-free series and $n = 20$ for the 6% lime-stabilized series, for a total of $n = 24$ data points. Multicollinearity among the variables was additionally examined through variance inflation factors (VIF).

3. Results and Discussion

3.1. Consistency Limits of the Mixtures

Figure 3 presents the Atterberg limits of kaolin as a function of VTW content, for both the lime-free series and the series stabilized with a constant 6% lime. In the lime-

free kaolin–VTW mixtures, the LL decreased from 32.5% for untreated kaolin to 28.9% at 20% VTW, with only minor changes observed at 10–15% VTW (≈30.4–30.8%) before a further reduction at 20% replacement. By comparison, the PL changed little and increased slightly from 21.7% to 22.1% at 20% VTW. Accordingly, the PI declined from 10.7% to 6.8% as VTW content increased, indicating reduced plastic behaviour in the lime-free series. The changes in Atterberg limits with increasing VTW content are consistent with the physical modification mechanisms widely reported for natural pozzolans and volcanic ash additives in fine-grained soils, particularly those classified as CL clays. The reduction in LL can be attributed to the dilution effect of non-plastic granular particles, which decrease the active clay fraction and lower the mixture's overall affinity for water [1,82]. Similar reductions have been observed in expansive clays stabilized with natural pozzolana and volcanic ash, where textural coarsening results in decreased water-holding capacity [44,83]. Although PL exhibited only a marginal increase [3], the marked decline in PI indicates improved workability and reduced plastic sensitivity of kaolin even in the absence of lime stabilization [84].

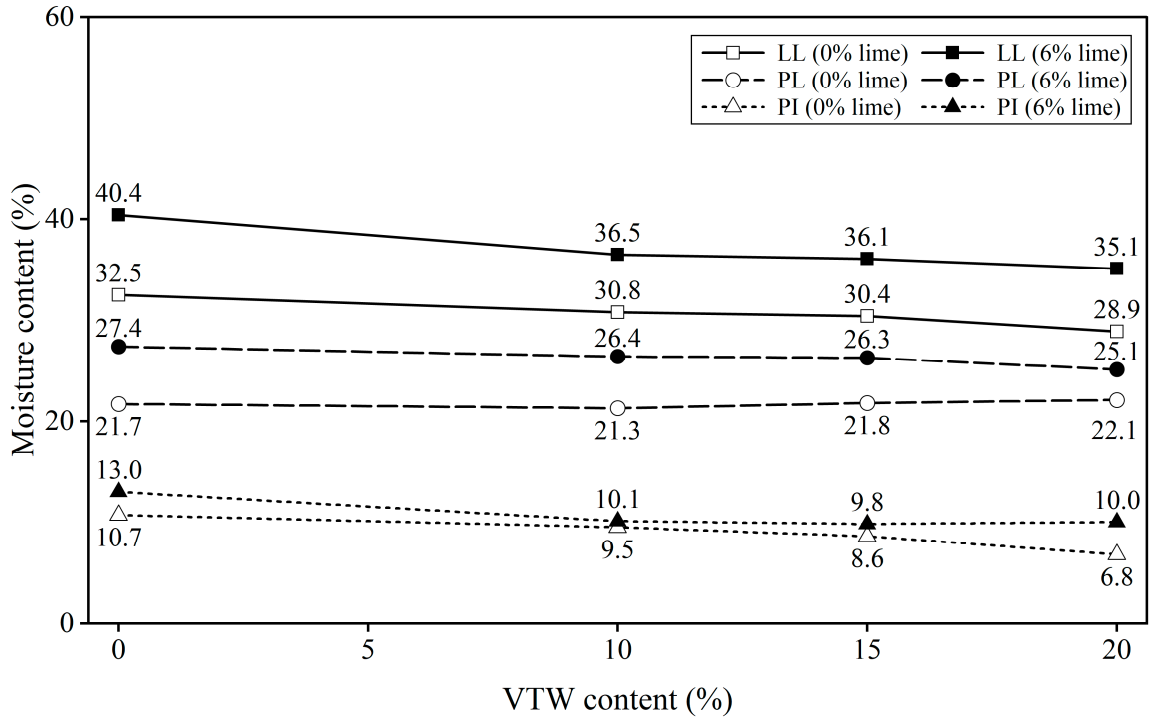


Figure 3. Variation in Atterberg limits (LL, PL, and PI) of kaolin as a function of VTW content for lime-free and 6% lime-stabilized mixtures.

As also shown in Figure 3, the series stabilized with a constant 6% lime dosage exhibited higher initial consistency limits than lime-free specimens. The LL increased to 40.4%, the PL to 27.4%, and the PI to 13.0%, reflecting the significant influence of lime stabilization on the soil's consistency behaviour. However, with the progressive addition of VTW, all consistency limits exhibited a decreasing tendency. The LL decreased from 40.4% to 35.1% as VTW content increased to 20%, while the PL declined from 27.4% to 25.1%. Consequently, the PI was reduced to 10.0%, indicating that VTW addition mitigated the elevated plasticity induced by lime and contributed to a less plastic response within the lime-stabilized system. Such increases in LL and PL following lime addition have been reported in fine-grained soils during the early stages of stabilization, where lime-induced flocculation alters the soil fabric and temporarily increases water demand [83,85]. In contrast, the subsequent decrease in LL and PI with increasing VTW content suggests

that VTW offsets the elevated plasticity associated with lime stabilization. This behaviour may be linked to the combined effects of physical dilution and the contribution of siliceous pozzolanic particles under alkaline conditions, promoting a less plastic and more workable soil structure over time [44,82].

3.2. Compaction Behaviour of the Mixtures

The compaction behaviour of the specimens is illustrated in Figure 4, showing the variation in MDD (Figure 4a) and OMC (Figure 4b) with VTW content for both 0% lime and 6% lime conditions. The addition of 6% lime reduced the MDD from 16.39 to 15.51 kN/m^3 and increased the OMC from 18.6% to 21.5%. This behaviour is generally associated with flocculation–agglomeration processes induced by lime, leading to a more open soil structure. Similar compaction responses in lime-stabilized clays have been widely documented in previous studies [25,34,86].

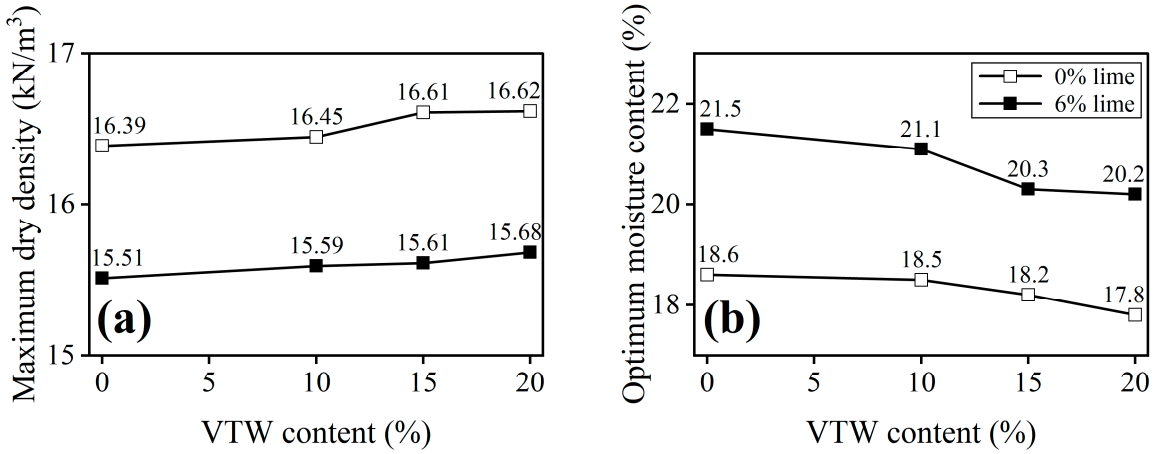


Figure 4. Compaction characteristics of kaolin–VTW mixtures with lime-free and 6% lime-stabilized conditions: (**a**) MDD; (**b**) OMC.

Increasing VTW content led to a gradual rise in MDD in the lime-free specimens, from 16.39 to 16.62 kN/m^3 (Figure 4a), indicating enhanced densification. Comparable densification effects in volcanic ash and zeolite-modified clays have been reported in the literature [5,48,49], where fine pozzolanic particles have been linked to a filler effect. In the 6% lime-stabilized specimens, VTW addition also increased MDD from 15.51 to 15.68 kN/m^3 (Figure 4a). This result indicates that VTW partially compensates for the density reduction associated with lime stabilization and is consistent with findings reported for lime–pozzolan mixtures [24,46].

A contrasting trend was observed for OMC (Figure 4b). While lime increased moisture demand, VTW incorporation reduced OMC in both lime-free and lime-stabilized specimens, decreasing from 21.5% to 20.2% in lime-stabilized specimens and from 18.6% to 17.8% in lime-free specimens. The increase in OMC following lime addition is commonly attributed to the additional moisture required for hydration reactions and cation exchange processes, which modify the soil's moisture retention behaviour [25,86]. In contrast, the reduction in OMC with VTW incorporation has been associated with the incorporation of non-plastic siliceous particles and their physical characteristics, such as angular morphology and relatively higher specific gravity, which facilitate enhanced densification at lower water contents [5,34,49].

3.3. Unconfined Compressive Strength (UCS) Behaviour of the Mixtures

The UCS behaviour of the studied mixtures was evaluated to distinguish the individual and combined effects of VTW addition, lime stabilization, and curing time. In this context,

strength development may be influenced by both physical filler effects and pozzolanic reactions [22,87,88]. Accordingly, the lime-free specimens were first assessed to clarify the role of VTW in the absence of a calcium source (Figure 5a), while the lime-stabilized specimens were subsequently examined to reveal the combined influence of lime, VTW, and curing duration on strength development (Figure 5b).

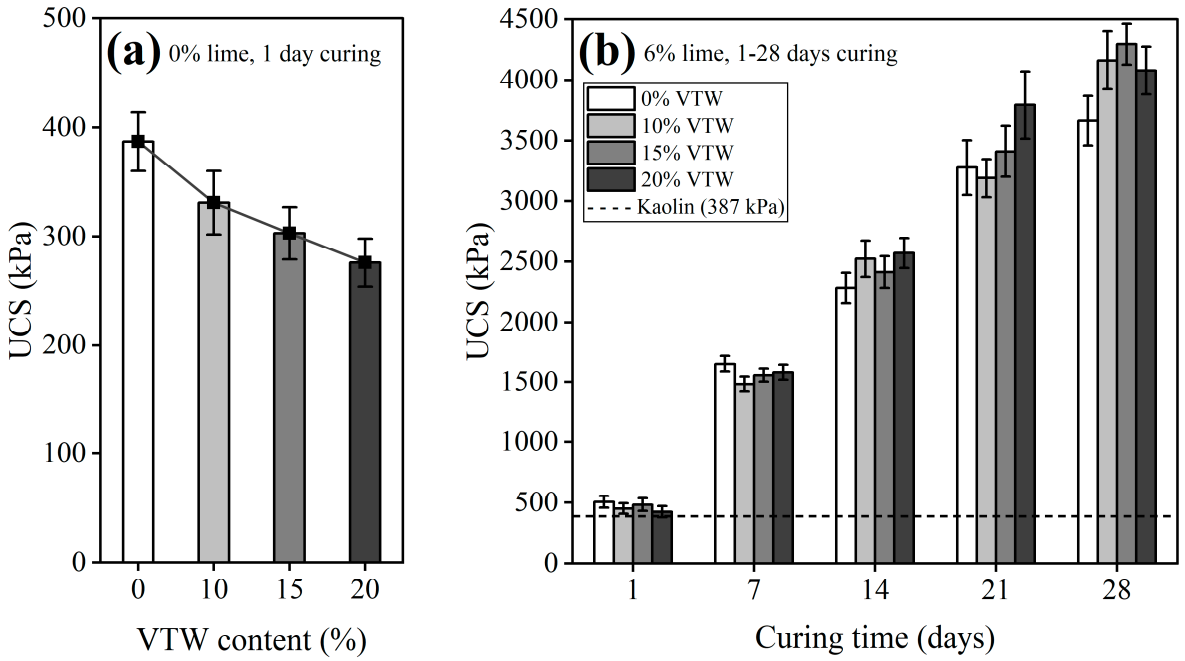


Figure 5. UCS of kaolin–VTW mixtures with VTW contents of 0%, 10%, 15%, and 20%: (**a**) lime-free specimens cured for 1 day; (**b**) 6% lime specimens cured for 1, 7, 14, 21, and 28 days. Each bar represents the mean of three replicates with error bars indicating ± 1 standard deviation. The dashed horizontal line in (**b**) represents the UCS of untreated kaolin (387 kPa).

Figure 5a shows the 1-day UCS values of the lime-free specimens containing different VTW contents. As the VTW content increased, the UCS gradually decreased from 387 kPa for untreated kaolin to 276 kPa at 20% VTW. Under lime-free conditions, the contribution of VTW is interpreted to be predominantly physical, since the absence of a calcium source limits the development of additional cementitious bonding. In this case, VTW mainly acts as a non-cementing mineral additive, and its increasing incorporation progressively reduces the proportion and continuity of the cohesive clay matrix. This dilution effect may weaken interparticle bonding and reduce the cohesive resistance of the specimens, thereby resulting in lower compressive strength [88–90].

Figure 5b presents the UCS values of the specimens containing 6% lime at curing periods of 1, 7, 14, 21, and 28 days. Compared with the corresponding lime-free mixtures, lime addition markedly enhanced strength development throughout the curing period (for example, at 1-day curing, the lime-only mixture reached 506 kPa, approximately 31% higher than the 387 kPa of untreated kaolin), consistent with previous studies on lime stabilization of clay soils [3,25,27,34,91].

At early curing (1 day), the mixtures containing VTW exhibited slightly lower UCS values than the lime-only mixture. This behaviour can be attributed to the short-term modification stage commonly observed in lime-stabilized clays, during which cation exchange and flocculation–agglomeration dominate the initial restructuring of the soil fabric [21,23,92]. At this stage, strength gain is mainly associated with physicochemical rearrangement among clay particles rather than the formation of substantial cementitious products [24,93]. Since pozzolanic reactions remain limited during this early period, VTW

functions primarily as a filler, and its contribution to strength development is therefore not yet pronounced [27,36].

With increasing curing time, however, the UCS values rose substantially for all lime-stabilized mixtures. Although the lime-only mixture showed the highest UCS at 7 days, the VTW-containing mixtures exceeded it from 14 days onward. This trend indicates that VTW likely became more effective at later curing stages. A possible explanation is that the alkaline environment provided by lime may have facilitated the gradual dissolution of reactive silica and alumina from VTW, thereby favouring pozzolanic interactions with calcium. Such reactions may have contributed to the progressive development of secondary cementitious products and, in turn, to improved interparticle bonding and strength [12,20,46,82,94–96].

Among the tested mixtures, the specimen containing 20% VTW achieved the highest UCS values at the intermediate curing stages, reaching 2572 kPa at 14 days and 3794 kPa at 21 days. At 28 days, however, the highest UCS was obtained for the mixture containing 15% VTW (4296 kPa), followed by the mixture containing 10% VTW (4162 kPa), while all VTW-containing mixtures still exhibited higher UCS values than the lime-only mixture (3664 kPa). Notably, the 28-day UCS of the 15% VTW mixture was approximately 17.2% higher than that of the lime-only mixture, highlighting the beneficial contribution of VTW when incorporated at an appropriate dosage. These findings suggest that although relatively high VTW contents may accelerate strength development during intermediate curing periods, long-term strength is governed by the presence of an optimum VTW content.

The change in the best-performing mixture with curing time reflects the balance between the calcium supplied by the fixed 6% lime and the reactive silica released from VTW. At intermediate ages, the higher silica content of the 20% VTW mixture sustains faster early pozzolanic gain, but as the finite calcium becomes limiting, its excess silica likely remains partly unreacted and restricts further strength development. The 15% VTW mixture maintains a more favourable calcium-to-silica balance through 28 days, confirming it as the optimum content at the curing age generally regarded as representative. This dosage-dependent behaviour, in which strength increases with additive content up to an optimum level and then decreases, is consistent with previous stabilization studies and is commonly attributed to the calcium-to-silica balance of the system [25,46,83,97–101].

3.4. California Bearing Ratio (CBR) Behaviour of the Mixtures

Figure 6 presents the CBR and CBR swell responses of the kaolin-based mixtures containing different VTW contents under lime-free and lime-stabilized conditions. As shown in Figure 6a, the lime-free mixtures exhibited generally low CBR values (3–8%) and did not show a systematic improvement trend with increasing VTW content. The non-monotonic response observed in the lime-free series, with the highest value (8%) at 15% VTW and lower values at intermediate dosages, likely reflects the limited contribution of VTW as a non-cementing filler in the absence of an alkaline activator, combined with potential variations in particle packing. This limited and irregular response suggests that VTW alone was insufficient to produce a meaningful enhancement in bearing resistance, which is consistent with previous studies reporting that additive-only stabilization generally results in only modest CBR improvement unless an effective binder or activator is present [102–104].

In contrast, the addition of 6% lime resulted in a marked increase in CBR, as also shown in Figure 6a. The CBR values of the lime-stabilized mixtures ranged from 43% to 80%, demonstrating a pronounced improvement relative to the lime-free mixtures. The highest CBR value of 80% was obtained at 15% VTW, indicating that this mixture provided the most pronounced bearing improvement. This marked increase indicates that the beneficial effect of VTW became pronounced only after lime addition, highlighting the importance of

calcium availability in mobilizing the stabilizing potential of the mixture. Similar behaviour has been reported in previous studies on lime-stabilized clayey soils and kaolin-based systems, where lime significantly increased CBR and more favourable performance was achieved when aluminosilicate or natural pozzolanic additives were incorporated together with lime [3,45,71,105]. However, the decline observed at 20% VTW suggests that the optimum VTW content for CBR improvement was exceeded. This behaviour is in line with studies showing that CBR may decrease beyond an optimum additive content when the binder-to-additive balance becomes less favourable and the efficiency of stabilization is reduced [3,102].

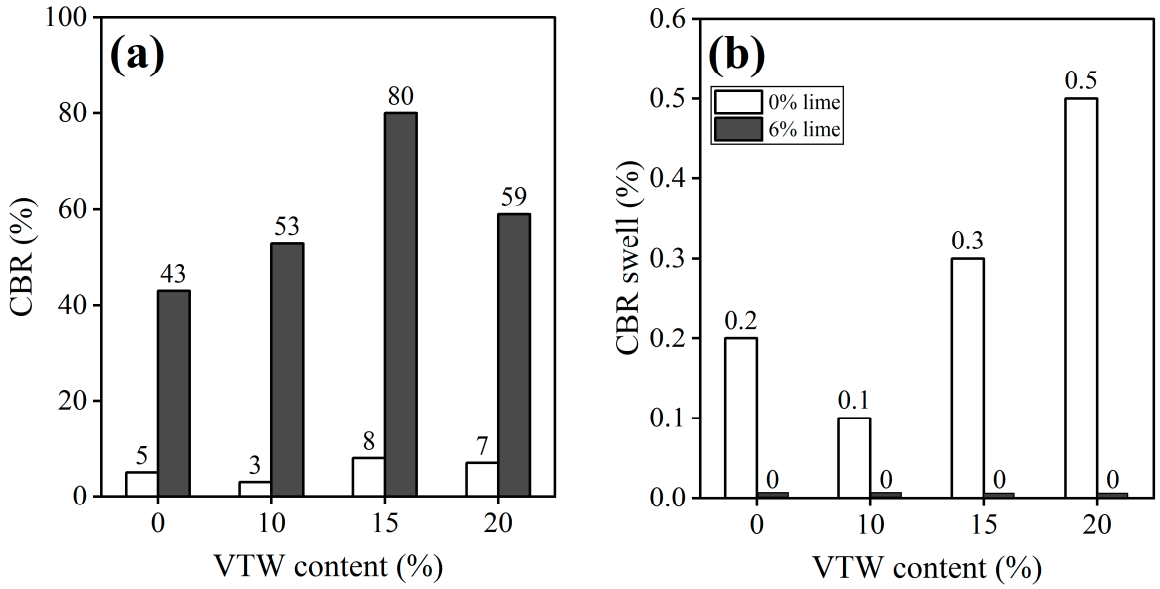


Figure 6. (**a**) CBR values and (**b**) CBR swell values of kaolin-based mixtures containing different VTW contents under lime-free and lime-stabilized conditions. Each bar represents the mean of three replicates.

As shown in Figure 6b, the CBR swell values of the lime-free mixtures varied between 0.1% and 0.5%, whereas no CBR swell was observed in the lime-stabilized mixtures. In absolute terms, these swell percentages correspond to height changes of approximately 0.12–0.58 mm for the lime-free mixtures, relative to the 116.4 mm initial specimen height, whereas the lime-stabilized mixtures exhibited no measurable height change (0.00 mm). This finding demonstrates that lime stabilization improved not only penetration resistance but also dimensional stability during soaking. Similar reductions in expansion or swell have been widely reported in lime-stabilized and lime–pozzolan-stabilized fine-grained soils, where cation exchange, flocculation–agglomeration, and subsequent pozzolanic reactions contribute to the development of a denser and less water-sensitive structure [32,45,106].

3.5. Mineralogical Characteristics of the Mixtures Based on XRD

Figure 7 presents the XRD patterns of kaolin, VTW, kaolin stabilized with 6% lime, and the optimum mixture (kaolin + 15% VTW + 6% lime). The kaolin pattern showed the characteristic reflections of kaolinite at around 2θ = 12.3° and 24.8°, together with the prominent quartz peak near 26.6°, while montmorillonite was also identified. Kaolinite- and quartz-dominated mineralogy has been widely reported for kaolinitic clays [46,86,100]. By contrast, VTW exhibited a heterogeneous mineral assemblage composed predominantly of feldspathic and silica-bearing phases, particularly plagioclase and K-feldspar, together with cristobalite, quartz, tridymite, and magnetite. Feldspathic minerals and silica polymorphs have likewise been identified as common constituents of volcanic tuffs and natural

pozzolans [48,49,59,107]. The diffractogram also displayed a broad diffuse background elevation between approximately 20° and 30° 2θ, suggesting the presence of a glassy or poorly crystalline component, which is often associated with the reactive fraction of volcanic pozzolanic materials [108,109]. Taken together, the coexistence of this reactive amorphous (glassy) fraction with a multi-phase crystalline assemblage reflects the glass-rich, multi-phase character that distinguishes ignimbritic tuff from more mineralogically uniform or fully altered volcanic-origin pozzolans such as zeolites. Beyond this distinction, the silica- and aluminosilicate-bearing constituents of VTW are expected to contribute to lime-mediated reactions [1,44,83,84].

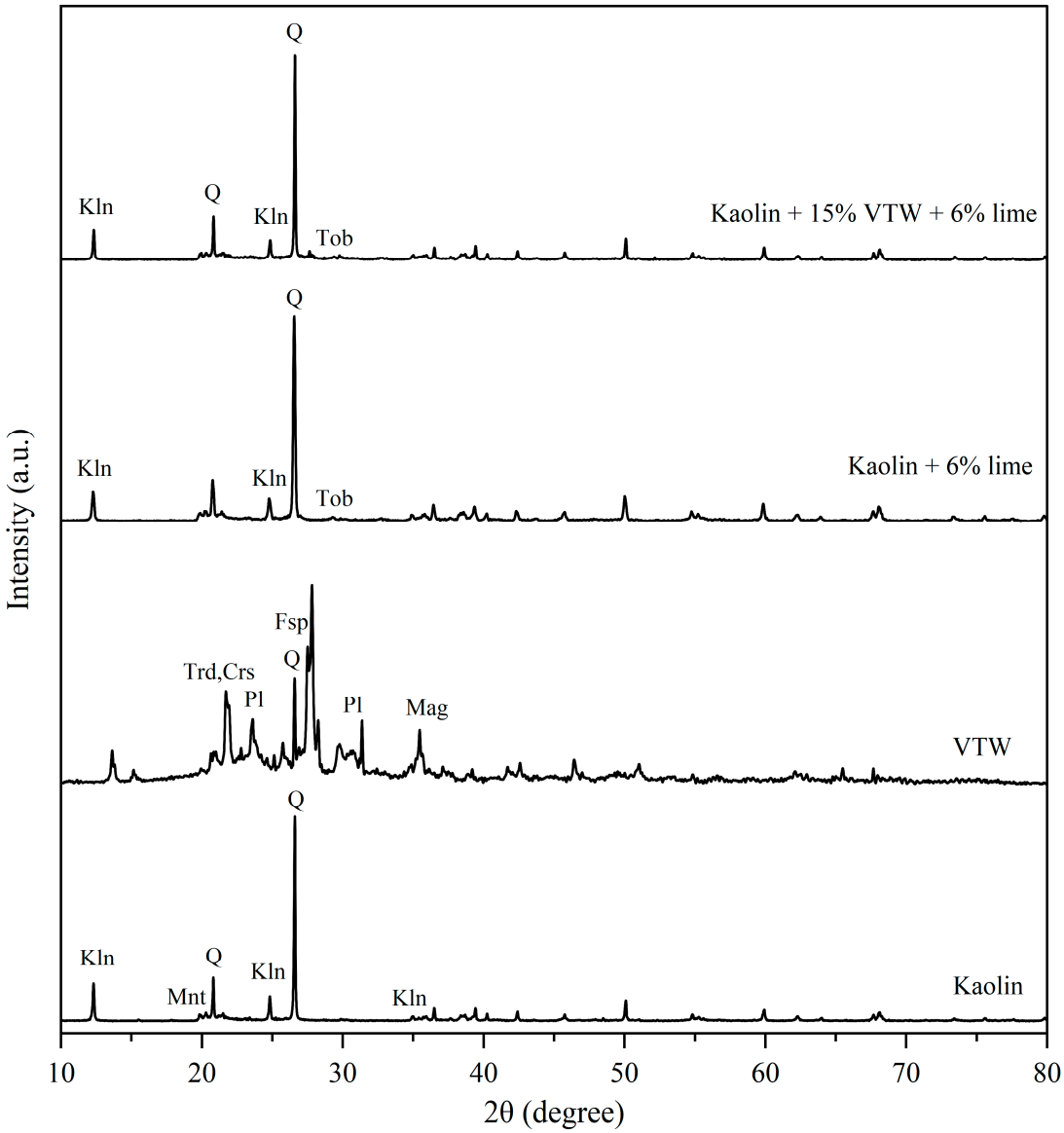


Figure 7. XRD patterns of kaolin, VTW, the lime-stabilized kaolin (kaolin + 6% lime), and the optimum mixture (kaolin + 15% VTW + 6% lime). Q: quartz; Kln: kaolinite; Mnt: montmorillonite; Pl: plagioclase; Fsp: feldspar; Crs: cristobalite; Trd: tridymite; Mag: magnetite; Tob: tobermorite.

In the lime-stabilized mixtures, the characteristic reflections of quartz, kaolinite, and montmorillonite remained discernible, indicating that the principal mineral framework of kaolin was largely retained after stabilization. However, compared with untreated kaolin, the kaolinite reflections, particularly those around 2θ = 12.3° and 24.8°, appeared less pronounced in the stabilized mixtures. Similar changes have been reported in lime-stabilized

clay and clay–pozzolan systems and have been attributed to the partial alteration and consumption of kaolinite during stabilization reactions [73,110]. In addition, phase-matching analysis of the lime-stabilized kaolin and the optimum mixture containing 15% VTW indicated the presence of Tobermorite 9 Å, a C-S-H-related crystalline phase that was not detected in untreated kaolin. The identification of Tobermorite 9 Å indicates the formation of cementitious reaction products during stabilization and supports the UCS behaviour discussed in Section 3.3 and presented in Figure 5. In the VTW-containing mixture, this finding may also reflect the contribution of reactive silica and alumina supplied by VTW, which could further promote stabilization reactions in the presence of lime [17,111]. The detection of Tobermorite 9 Å in the optimum mixture provides mineralogical support for the enhanced stabilization observed at 15% VTW, suggesting that this dosage promotes a favourable balance between lime and reactive silica/alumina, conducive to effective interparticle bonding [25].

3.6. Chemical Bonding Characteristics of the Mixtures Based on FTIR

FTIR analysis was used to evaluate the chemical interactions developed during stabilization and to identify possible reaction products through changes in hydroxyl-, carbonate-, and silicate/aluminosilicate-related bands [112]. As a complementary characterization technique, FTIR is useful for monitoring both crystalline and amorphous phases in cementitious and clay-based systems [113]. As shown in Figure 8, the spectra include kaolin and lime (Figure 8a); the kaolin + 6% lime mixture compared with kaolin and lime (Figure 8b); kaolin, lime, and VTW (Figure 8c); and the overall comparison of kaolin, lime, and VTW with the stabilized mixtures containing 15% VTW (Figure 8d).

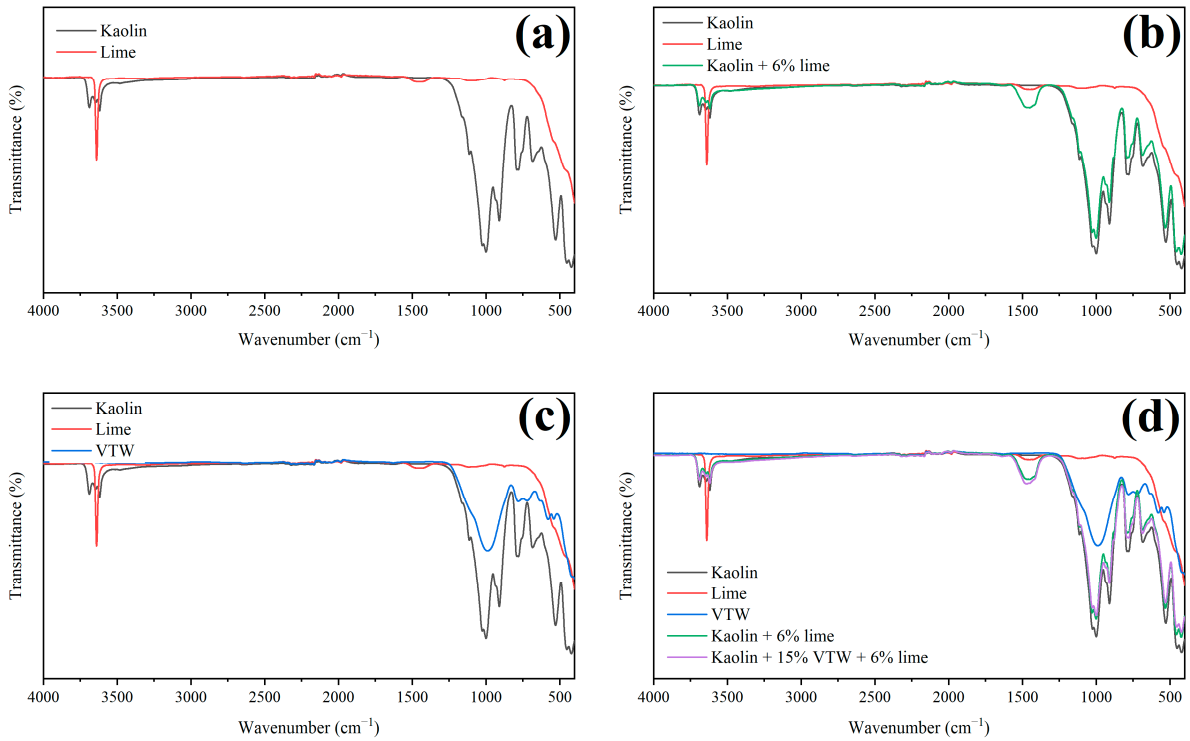


Figure 8. FTIR spectra of kaolin, lime, VTW, and stabilized mixtures: (**a**) kaolin and lime; (**b**) kaolin + 6% lime mixture with kaolin and lime; (**c**) kaolin, lime, and VTW; (**d**) overall comparison of kaolin, lime, VTW, and stabilized mixtures containing 15% VTW.

The sharp bands observed at 3689.16, 3646.73, and 3619.73 cm^{-1} in untreated kaolin are assigned to the characteristic OH stretching vibrations of kaolinite (Figure 8a). The persistence of these bands in the lime-stabilized and VTW-containing mixtures

(Figure 8b,d) indicates that the main kaolinite framework remained largely preserved during stabilization [46,86,114]. In the 1400–1500 cm^{-1} region, the band observed at 1451.17 cm^{-1} in the kaolin + 6% lime mixture remained evident, whereas it shifted to 1470.46 cm^{-1} in the kaolin + 15% VTW + 6% lime mixture (Figure 8b,d). A direct comparison with the reference spectra of the raw materials supports the origin of this band: the 1451 cm^{-1} band coincides with the carbonate band of the raw hydrated lime, while kaolin and VTW are essentially featureless in this region (Figure 8). This change is consistent with carbonation-related CO_3^{2-} vibrations reported for lime-containing mixtures and indicates that the carbonate environment is modified in the presence of VTW rather than by the lime alone, with part of the available calcium involved in carbonate formation during stabilization [113,115,116]. The assignments of the main FTIR bands for all samples, based on the reference spectra and the literature, are summarized in Table 5. The main spectral changes were observed in the 900–1150 cm^{-1} region, where the bands at 1024.02 and 999.91 cm^{-1} in untreated kaolin are attributed to Si–O stretching vibrations (Figure 8c). After the addition of lime and VTW, noticeable changes in the position and profile of these bands were observed in the stabilized mixtures (Figure 8d), indicating modifications in the silicate/aluminosilicate bonding environment during stabilization [117,118]. In the fingerprint region below 900 cm^{-1}, the bands around 780.06 and 686.53 cm^{-1} are associated with quartz- and kaolinite-related vibrations, whereas the bands near 530.32 and 454.15 cm^{-1} are attributed to Si–O–Al and Si–O/Si–O–Si vibrations in the aluminosilicate framework (Figure 8c,d). The persistence of these low-wavenumber bands after lime and VTW addition indicates that, although stabilization modified the bonding environment, the fundamental silicate/aluminosilicate framework of the system remained detectable [18,119].

Table 5. Assignment of the main FTIR bands of the raw materials and stabilized mixtures, based on reference spectra and the literature.

Wavenumber (cm^{-1})	Assignment	Observed in	References
3689, 3647, 3620	O–H stretching (kaolinite inner and inner-surface hydroxyls)	Kaolin; retained in all stabilized mixtures	[46,86,114]
1470/1451	CO_3^{2-} stretching (carbonation); 1451 in lime and lime-only mixture, shifted to 1470 in VTW-bearing mixtures	1451: lime, kaolin + 6% lime; 1470: kaolin + 15% VTW + 6% lime	[113,115,116]
1024, 1000	Si–O stretching (kaolinite)	Kaolin; modified in stabilized mixtures	[117,118]
~780, ~686	Quartz- and kaolinite-related vibrations	All samples	[18,119]
~530	Si–O–Al bending	All samples	
~454	Si–O/Si–O–Si bending	All samples	

3.7. Microstructural Characteristics of the Mixtures Based on SEM

Figure 9 presents the SEM images of (a) untreated kaolin, (b) kaolin stabilized with 6% lime, and (c) kaolin stabilized with 6% lime and 15% VTW.

The SEM image of untreated kaolin (Figure 9a) reveals the characteristic platy, book-like morphology of kaolinite particles, which are stacked along their basal surfaces to form well-developed aggregates and locally compact assemblages [120–123]. Micropores are observed at irregular boundaries where aggregates of different orientations intersect. In localized regions, features indicative of pseudohexagonal morphology are also visible, consistent with the crystallographic growth characteristics commonly reported for kaolinite [124,125].

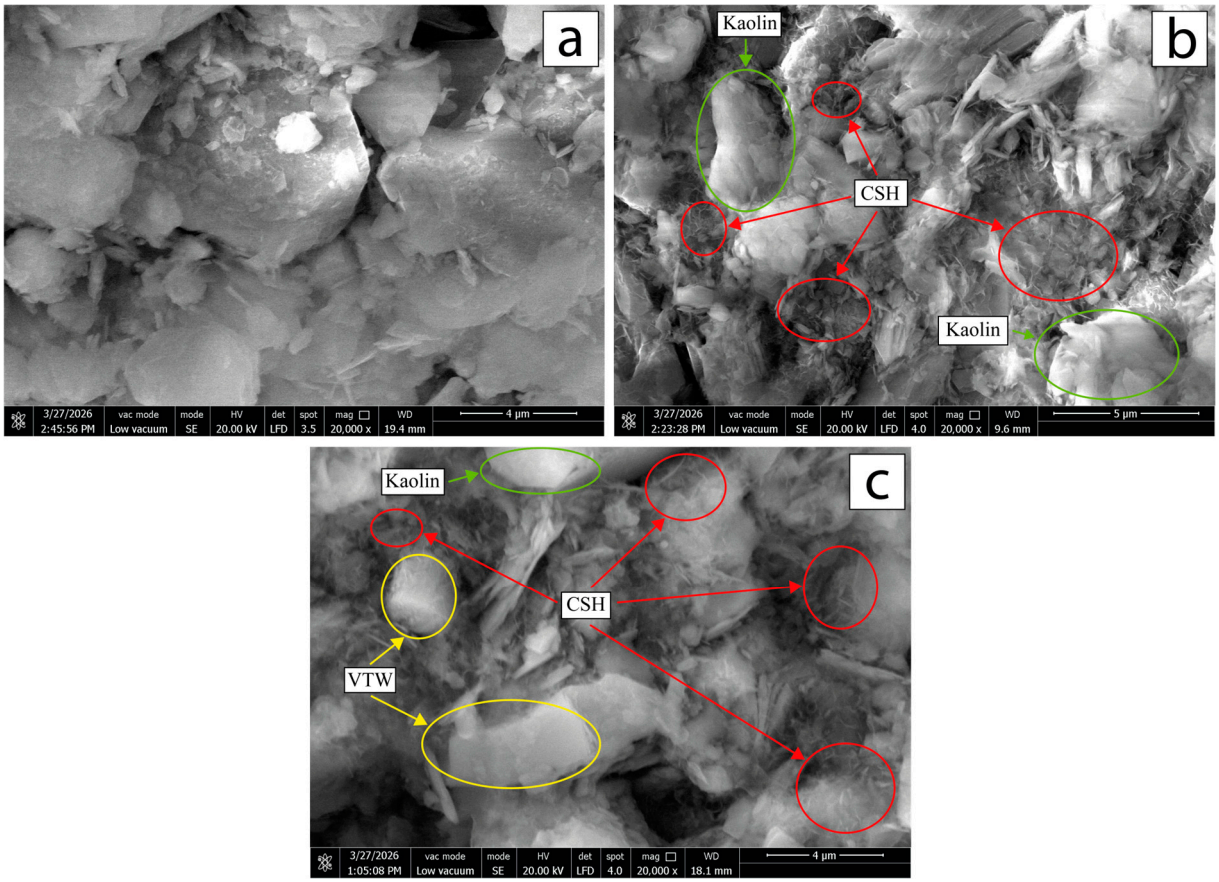


Figure 9. SEM images of (**a**) untreated kaolin, (**b**) kaolin stabilized with 6% lime, and (**c**) kaolin stabilized with 6% lime and 15% VTW.

The addition of 6% lime results in pronounced microstructural reorganization (Figure 9b), characterized by the development of fine, fibrous, and reticulated morphologies that fill interparticle voids and coat the surfaces of coarser particles. Such network-like features are attributed to calcium silicate hydrate (C–S–H) gel formation in lime-stabilized systems [46,92,126]. The progressive infilling of pore spaces suggests the development of a more cohesive and continuous matrix. Coarser platy structures observed in several regions are attributed to partially unreacted kaolinite particles. An interlocking fabric between gel-like phases and residual particles is evident, indicating a denser microstructure compared to the untreated kaolin. These observations are consistent with the mineralogical and chemical changes identified by XRD and FTIR analyses, collectively indicating the formation of pozzolanic reaction products in the lime-stabilized system.

The incorporation of 15% VTW leads to further microstructural modifications (Figure 9c). The microstructure is characterized by the presence of coarse, angular particles associated with VTW, representing a shift from the gel-dominated structure observed in the lime-only sample. Fine, short-stranded morphologies at the interparticle contact zones are consistent with the localized development of C–S–H gel phases [34,46]. In some regions, VTW particle surfaces appear to partially obscure the underlying gel structures. Despite the more heterogeneous appearance, the resulting interlocking configuration suggests an effective particle arrangement, consistent with the improved mechanical performance observed for the 15% VTW mixture. The concurrence of these features with the XRD and FTIR results collectively indicates that VTW enhances the development of pozzolanic reaction products within the lime-stabilized matrix.

3.8. Correlation Analysis of Geotechnical Parameters

To better understand the interactions among the measured parameters, a Pearson correlation analysis was performed (Figure 10), and a multicollinearity diagnosis is summarized in Table 6.

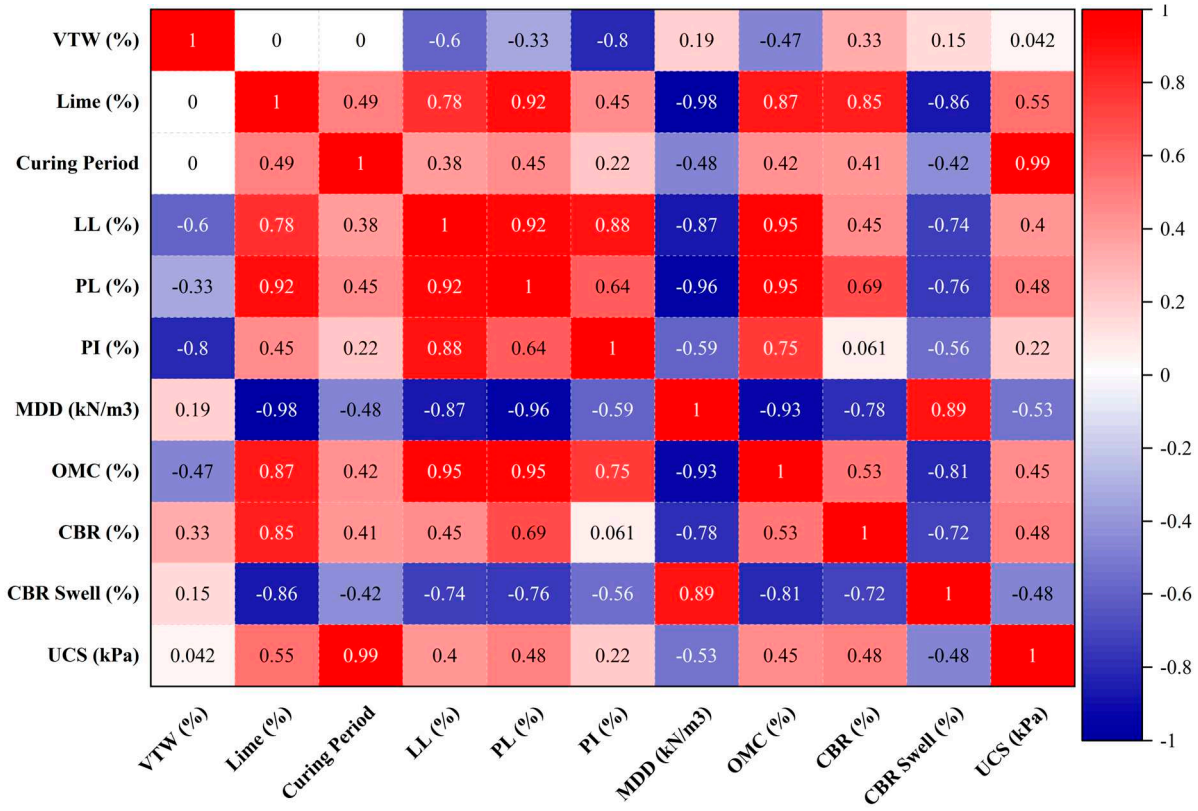


Figure 10. Pearson correlation matrix illustrating the relationships among plasticity, compaction, strength, and bearing capacity parameters of the kaolin–VTW–lime mixtures.

Table 6. Variance inflation factors (VIF) and tolerance values for the experimental design variables (VTW content, lime content, and curing period) used in the multicollinearity diagnosis.

Design Variable	Tolerance	VIF
VTW content	1	1
Lime content	0.761	1.314
Curing period	0.761	1.314

VTW content exhibited statistically significant negative correlations with the plasticity-related parameters, with correlation coefficients of $r = -0.60$ ($p = 0.002$) for LL and $r = -0.80$ ($p < 0.001$) for PI, indicating a reduction in plasticity with increasing VTW content. Lime content showed strong, statistically significant correlations with several engineering properties, including MDD ($r = -0.98$, $p < 0.001$), OMC ($r = 0.87$, $p < 0.001$), and CBR ($r = 0.85$, $p < 0.001$). These relationships reflect the dual role of lime in modifying the soil fabric through cation exchange and flocculation–agglomeration and in promoting cementitious bonding through pozzolanic reactions. The most pronounced association with UCS was that of curing period ($r = 0.99$, $p < 0.001$), highlighting the time-dependent development of strength governed by the pozzolanic reaction, whereas lime content was also significantly correlated with UCS ($r = 0.55$, $p = 0.006$). In contrast, the correlation between VTW content and UCS was weak and not statistically significant ($r = 0.04$, $p = 0.845$), indicating that VTW influences plasticity and compaction rather than directly governing strength. CBR swell

exhibited statistically significant negative correlations with lime content ($r = -0.86$), CBR ($r = -0.72$), and UCS ($r = -0.48$), consistent with the reduced swelling potential of the stabilized specimens accompanying their improved strength and bearing capacity. Overall, these results indicate that VTW predominantly influences plasticity and compaction through physical mechanisms, whereas lime and curing govern strength and bearing performance through combined physico-chemical and pozzolanic processes.

Because several of these parameters are physically or definitionally interrelated (for example, PI = LL − PL, and the index and compaction parameters derive from the same mixture compositions), a multicollinearity diagnosis was carried out. When all candidate variables were entered together, near-perfect linear dependencies produced very high, effectively undefined variance inflation factors, confirming that these variables should not be treated as independent predictors. When only the experimental design variables were considered (VTW content, lime content, and curing period), the variance inflation factors were low (1.00–1.31; Table 6), indicating no multicollinearity among the primary design factors. Accordingly, the Pearson coefficients reported here are interpreted as descriptive measures of association rather than as independent or causal predictors of the measured properties.

4. Conclusions

The following conclusions can be drawn from this study:

1. In lime-free mixtures, VTW addition reduced the plasticity index from 10.7% to 6.8% at 20% VTW, indicating improved workability even without lime stabilization. In lime-stabilized mixtures, VTW mitigated the increase in plasticity induced by lime, reducing the PI from 13.0% to 10.0% at 20% VTW.
2. VTW incorporation slightly increased the MDD (from 16.39 to 16.62 kN/m^3 in lime-free mixtures and from 15.51 to 15.68 kN/m^3 in lime-stabilized mixtures) while reducing the OMC, suggesting a filler effect that promotes more efficient particle packing.
3. Under lime-free conditions, UCS decreased with increasing VTW content at 1-day curing (from 387 to 276 kPa as VTW increased from 0% to 20%), indicating that VTW primarily acts as a non-cementing filler in the absence of a calcium source, and that significant pozzolanic activity is not expected without an alkaline environment. In contrast, lime-stabilized mixtures exhibited substantial strength development with curing time, with all VTW-containing mixtures surpassing the lime-only mixture from 14 days onward.
4. The mixture containing 15% VTW achieved the highest 28-day UCS of 4296 kPa, corresponding to an increase of approximately 17.2% compared to the lime-only mixture, indicating that 15% VTW represents the optimum content for long-term strength development.
5. CBR results further supported the optimum VTW content of 15%, yielding the highest CBR value of 80% among lime-stabilized mixtures. No CBR swell was observed in any lime-stabilized mixture, indicating improved volumetric stability during soaking.
6. XRD analysis indicated the formation of Tobermorite 9 Å in lime-stabilized mixtures, providing mineralogical evidence of cementitious product development. FTIR analysis suggested modifications in the silicate/aluminosilicate bonding environment consistent with pozzolanic interactions, while SEM observations showed the development of C–S–H gel morphologies and interlocking microstructural features.
7. Pearson correlation analysis confirmed statistically significant negative correlations of VTW content with the plasticity parameters ($r = -0.80$ with PI, $p < 0.001$), significant correlations of lime content with the compaction and bearing capacity parameters ($r = -0.98$ with MDD, $r = 0.87$ with OMC, and $r = 0.85$ with CBR; all $p < 0.001$),

and a very strong positive correlation between curing period and UCS (r = 0.99, $p < 0.001$), confirming the dominant role of time-dependent pozzolanic reactions in strength development.

8. Taken together, 15% VTW was identified as the optimum content, beyond which the balance between available calcium and reactive silica becomes less favourable, potentially limiting further cementitious product formation and strength gain.

Beyond the individual test results, the combined findings indicate that lime–VTW stabilization simultaneously improves three independent aspects of soil behaviour: workability (through reduced plasticity), load-bearing capacity (through UCS and CBR gains), and volumetric stability (through the absence of CBR swell during soaking). This combination is particularly relevant for fine-grained subgrade soils, where inadequate strength and moisture-induced volume change typically coexist. The CBR value of 80% obtained at 15% VTW reflects a bearing capacity well above the levels generally required for stabilized subgrade layers, while the elimination of swelling addresses the volumetric instability that commonly limits the use of clayey soils in road subgrades, embankments, and shallow foundation support. On this basis, lime-stabilized kaolin incorporating VTW at its optimum content of 15% can be regarded as a technically promising and resource-efficient option for subgrade improvement and similar ground-improvement applications, with a recommended starting dosage of 6% lime and 15% VTW for comparable fine-grained soils, pending field-scale verification under service conditions.

5. Limitations and Future Research

Despite the comprehensive experimental program adopted in this study, several limitations should be acknowledged. First, kaolin was selected as a model soil to minimize mineralogical variability and ensure reproducibility of the experimental outcomes; therefore, the findings may require further validation when applied to natural clay soils with more complex mineralogical compositions and varying organic content. Second, the experimental program was conducted under controlled laboratory conditions, and the long-term durability of the stabilized mixtures under environmental exposure (such as wet–dry and freeze–thaw cycling) was not investigated. A related durability consideration concerns the potential for alkali–silica reaction (ASR), since VTW combines a high silica content with appreciable alkali oxides (K_2O and Na_2O), and lime provides a high-pH environment. Several factors, however, suggest that this risk is limited in the present system: the reactive silica and alumina supplied by VTW are largely consumed through pozzolanic reactions to form C–S–H and related cementitious phases together with Tobermorite, as confirmed by the XRD, SEM, and FTIR analyses, so that silica bound into these phases is not available to form expansive ASR gel. Consistent with this, no swelling was recorded in the lime-stabilized mixtures during the soaked CBR tests, indicating that expansive reactions were not manifested under the conditions examined. A further environmental consideration concerns the potential leaching of trace elements from VTW. Although direct leachate testing of the stabilized mixtures was not undertaken in this study, two factors suggest that this risk is limited. A TCLP-based assessment of pyroclastic materials from the same Nemrut volcanic system—including Ahlat stone, the very ignimbritic tuff from which VTW is derived as a cutting by-product—reported structurally stable behaviour with heavy-metal release well below the relevant USEPA and national limits even under aggressive leaching conditions [127]. In addition, the high-pH environment and the C–S–H and Tobermorite phases formed during lime–VTW reaction are recognized mechanisms for immobilizing trace metals within a cementitious matrix, consistent with the very low SO_3 content of VTW. Direct leachate characterization nonetheless remains necessary to confirm environmental compatibility under service conditions. Third, the study focused

on subgrade-relevant performance parameters; field-scale validation under actual traffic loading and real environmental conditions remains to be addressed.

Building on these findings, future research should extend the present results to clay soils with different mineralogical compositions, investigate the long-term durability of VTW-stabilized systems under wet–dry and freeze–thaw cycling—including dedicated assessment of alkali–silica reaction and long-term expansion through accelerated mortar-bar testing or extended field monitoring—and assess the field-scale performance of VTW-stabilized subgrade applications. Furthermore, the optimum VTW content may shift depending on the specific calcium-to-silica balance required by different soil types, suggesting that future studies could explore the applicability of VTW across a broader range of clay mineralogies.

Author Contributions: Conceptualization, B.D. and Ö.Ç.; Methodology, H.İ.G. and Ö.Ç.; Software, B.D.; Validation, B.D. and H.İ.G.; Formal analysis, H.İ.G.; Investigation, B.D. and H.İ.G.; Resources, B.D.; Data curation, B.D. and Ö.Ç.; Writing—original draft, B.D. and H.İ.G.; Writing—review & editing, H.İ.G. and Ö.Ç.; Visualization, H.İ.G.; Supervision, Ö.Ç. All authors have read and agreed to the published version of the manuscript.

Funding: This research received no external funding.

Institutional Review Board Statement: Not applicable.

Informed Consent Statement: Not applicable.

Data Availability Statement: Data will be made available on request.

Conflicts of Interest: The authors declare no conflict of interest.

References

1. Al-Swaidani, A.; Hammoud, I.; Meziab, A. Effect of adding natural pozzolana on geotechnical properties of lime-stabilized clayey soil. *J. Rock Mech. Geotech. Eng.* **2016**, *8*, 714–725. [CrossRef]
2. Luo, Y.; Meng, J.; Wang, D.; Jiao, L.; Xue, G. Experimental study on mechanical properties and microstructure of metakaolin based geopolymer stabilized silty clay. *Constr. Build. Mater.* **2022**, *316*, 125662. [CrossRef]
3. Abdelbaset, A.M.; Katunský, D.; Zeleňáková, M.; El-Feky, M.H. Mechanical properties stabilization of low plasticity Kaolin soil using fly ash and hydrated lime. *Case Stud. Constr. Mater.* **2024**, *21*, e03662. [CrossRef]
4. Consoli, N.C.; Festugato, L.; Filho, H.C.S.; Miguel, G.D.; Neto, A.T.; Andreghetto, D. Durability Assessment of Soil-Pozzolan-Lime Blends through Ultrasonic-Pulse Velocity Test. *J. Mater. Civ. Eng.* **2020**, *32*, 04020223. [CrossRef]
5. MolaAbasi, H.; Kharazmi, P.; Khajeh, A.; Saberian, M.; Jamshidi Chenari, R.; Harandi, M.; Li, J. Low plasticity clay stabilized with cement and zeolite: An experimental and environmental impact study. *Resour. Conserv. Recycl.* **2022**, *184*, 106408. [CrossRef]
6. Khaiyum, M.Z.; Sarker, S.; Kabir, G. Evaluation of Carbon Emission Factors in the Cement Industry: An Emerging Economy Context. *Sustainability* **2023**, *15*, 15407. [CrossRef]
7. Perri, G.; De Rose, M.; Domitrović, J.; Vaiana, R. CO_2 Impact Analysis for Road Embankment Construction: Comparison of Lignin and Lime Soil Stabilization Treatments. *Sustainability* **2023**, *15*, 1912. [CrossRef]
8. Mosly, I. Carbon Footprint of Global Construction Industries: A Cross-Country Analysis of Emissions, Drivers, and the Construction Carbon Sustainability Index (1990–2023). *Sustainability* **2025**, *17*, 9274. [CrossRef]
9. Li, Q.; Li, Q.; Wu, J.; He, K.; Xia, Y.; Liu, J.; Wang, F.; Cheng, Y. Wellhead Stability During Development Process of Hydrate Reservoir in the Northern South China Sea: Sensitivity Analysis. *Processes* **2025**, *13*, 1630. [CrossRef]
10. Eades, J.L.; Grim, R.E. Reaction of hydrated lime with pure clay minerals in soil stabilization. *Highw. Res. Board Bull.* **1960**, 51–63.
11. Sherwood, P. *Soil Stabilization with Cement and Lime*; Her Majesty Stationary Office: Norwich, UK, 1993.
12. Barman, D.; Dash, S.K. Stabilization of expansive soils using chemical additives: A review. *J. Rock Mech. Geotech. Eng.* **2022**, *14*, 1319–1342. [CrossRef]
13. Pandey, V.K.; Dhiman, S.; Bharti, K. A review on the use of lime in soil stabilization. In *Latest Trends in Engineering and Technology*; CRC Press: Boca Raton, FL, USA, 2024; pp. 414–421. [CrossRef]
14. Anburuvel, A. The Engineering Behind Soil Stabilization with Additives: A State-of-the-Art Review. *Geotech. Geol. Eng.* **2024**, *42*, 1–42. [CrossRef]
15. Bell, F.G. Lime stabilization of clay minerals and soils. *Eng. Geol.* **1996**, *42*, 223–237. [CrossRef]

16. Di Sante, M.; Fratalocchi, E.; Mazzieri, F.; Pasqualini, E. Time of reactions in a lime treated clayey soil and influence of curing conditions on its microstructure and behaviour. *Appl. Clay Sci.* **2014**, *99*, 100–109. [CrossRef]
17. Jalal, F.E.; Xu, Y.; Jamhiri, B.; Memon, S.A. On the recent trends in expansive soil stabilization using calcium-based stabilizer materials (CSMs): A comprehensive review. *Adv. Mater. Sci. Eng.* **2020**, *2020*, 1510969. [CrossRef]
18. Eisazadeh, A.; Kassim, K.A.; Nur, H. Solid-state NMR and FTIR studies of lime stabilized montmorillonitic and lateritic clays. *Appl. Clay Sci.* **2012**, *67–68*, 5–10. [CrossRef]
19. Jha, A.K.; Sivapullaiah, P.V. Lime Stabilization of Soil: A Physico-Chemical and Micro-Mechanistic Perspective. *Indian Geotech. J.* **2020**, *50*, 339–347. [CrossRef]
20. Maddalena, R.; Li, K.; Chater, P.A.; Michalik, S.; Hamilton, A. Direct synthesis of a solid calcium-silicate-hydrate (C-S-H). *Constr. Build. Mater.* **2019**, *223*, 554–565. [CrossRef]
21. Rosone, M.; Megna, B.; Celauro, C. Analysis of the chemical and microstructural modifications effects on the hydro-mechanical behaviour of a lime-treated clay. *Int. J. Geotech. Eng.* **2021**, *15*, 447–460. [CrossRef]
22. Wu, J.; Liao, H.; Ma, Z.; Song, H.; Cheng, F. Effect of Different Initial CaO/SiO_2 Molar Ratios and Curing Times on the Preparation and Formation Mechanism of Calcium Silicate Hydrate. *Materials* **2023**, *16*, 717. [CrossRef] [PubMed]
23. Muhmed, A.; Wanatowski, D. Effect of lime stabilisation on the strength and microstructure of clay. *IOSR J. Mech. Civ. Eng.* **2013**, *6*, 87–94. [CrossRef]
24. Khajeh, A.; Jamshidi Chenari, R.; Payan, M.; MolaAbasi, H. Assessing the effect of lime-zeolite on geotechnical properties and microstructure of reconstituted clay used as a subgrade soil. *Phys. Chem. Earth Parts A/B/C* **2023**, *132*, 103501. [CrossRef]
25. Cimen, O.; Keles, E. Using fly ash and volcanic tuff along with lime for stabilizing high plasticity clay soil. *J. Fac. Eng. Archit. Gazi Univ.* **2025**, *40*, 1247–1258.
26. Li, S.; Liu, S.; Zhang, T.; Wang, Z.; Zhao, W. Experimental study on the durability and microstructural characteristics of lime-stabilized silty clay in seasonally frozen region. *Constr. Build. Mater.* **2025**, *463*, 140158. [CrossRef]
27. Deepak, M.S.; Rohini, S.; Harini, B.S.; Ananthi, G.B.G. Influence of fly-ash on the engineering characteristics of stabilised clay soil. *Mater. Today Proc.* **2021**, *37*, 2014–2018. [CrossRef]
28. Jeremiah, J.J.; Abbey, S.J.; Booth, C.A.; Kashyap, A. Behaviour and Microstructural Characteristics of Lime-GGBS-Treated Kaolin Clay Contaminated with Gypsum. *Materials* **2023**, *16*, 874. [CrossRef] [PubMed]
29. Anggraini, M.; Setiawan, D.M.; Saleh, A. Chemical stabilization techniques for clay soil: A comprehensive review. *J. Mech. Behav. Mater.* **2025**, *34*, 20250056. [CrossRef]
30. Firoozi, A.A.; Guney Olgun, C.; Firoozi, A.A.; Baghini, M.S. Fundamentals of soil stabilization. *Int. J. Geo-Eng.* **2017**, *8*, 26. [CrossRef]
31. Abeysinghe, A.M.S.N.; Kurukulasuriya, L.C.; Nasvi, M.C.M. A comparative assessment of geotechnical performance, cost and carbon footprint of expansive soil treated with cement, lime and fly ash. *Geomech. Geoengin.* **2025**, *20*, 937–955. [CrossRef]
32. Ji-ru, Z.; Xing, C. Stabilization of expansive soil by lime and fly ash. *J. Wuhan Univ. Technol.-Mater. Sci. Ed.* **2002**, *17*, 73–77. [CrossRef]
33. Singh, D.; Manojkumar, D.; Kumar, S. Strength characteristics of kaolin clay mixed with RHA, sand and lime. *Mater. Today Proc.* **2022**, *60*, 328–335. [CrossRef]
34. Zaini, M.S.I.; Hasan, M.; Almuaythir, S.; Hyodo, M. Experimental investigations on physico-mechanical properties of kaolinite clay soil stabilized at optimum silica fume content using clamshell ash and lime. *Sci. Rep.* **2024**, *14*, 10995. [CrossRef] [PubMed]
35. Sun, Y.; Li, C.; Bi, Q.; Li, J.; Zhang, J.; Lu, X.; Yang, Y. Experimental study and machine learning prediction on compressive strength of industrial waste- solidified marine soft soil under dry-wet cycles. *Case Stud. Constr. Mater.* **2025**, *23*, e04943. [CrossRef]
36. Aminaee, A.; Ardakani, A.; Baghbani, A.; Abuel-Naga, H.; Daghistani, F. Hybrid ML–XAI Framework for Predicting and Interpreting the Strength of Lime–Silica Fume Stabilized Clay for Sustainable Construction Applications. *Buildings* **2026**, *16*, 953. [CrossRef]
37. Shinde, B.; Sangale, A.; Pranita, M.; Sanagle, J.; Roham, C. Utilization of waste materials for soil stabilization: A comprehensive review. *Prog. Eng. Sci.* **2024**, *1*, 100009. [CrossRef]
38. Miller, S.A. Supplementary cementitious materials to mitigate greenhouse gas emissions from concrete: Can there be too much of a good thing? *J. Clean. Prod.* **2018**, *178*, 587–598. [CrossRef]
39. Munro, D.; Di Benedetto, G.; Graham, M.; Jans-Singh, M.; Turpin, M.; Kanavaris, F. The assessment of the embodied carbon of resource-constrained materials including ground granulated blast-furnace slag (GGBS) and ferrous scrap. *Structures* **2025**, *78*, 109175. [CrossRef]
40. Whittle, J.W.; Rihner, M.C.S.; Hafez, H.; Espinosa, R.M.E.; Fletcher, D.I.; Walkley, B.; Koh, L.S.C. From symbiosis to scarcity: Evaluating disruption associated with decarbonisation to circular waste materials between the UK cement and steel sectors. *Resour. Conserv. Recycl.* **2026**, *224*, 108560. [CrossRef]
41. Celik, K.; Meral, C.; Mancio, M.; Mehta, P.K.; Monteiro, P.J.M. A comparative study of self-consolidating concretes incorporating high-volume natural pozzolan or high-volume fly ash. *Constr. Build. Mater.* **2014**, *67*, 14–19. [CrossRef]

42. Shukla, A.; Gupta, N.; Gupta, A.; Goel, R.; Kumar, S. Natural Pozzolans a Comparative Study: A Review. *IOP Conf. Ser. Mater. Sci. Eng.* **2020**, *804*, 012040. [CrossRef]
43. Lemougna, P.N.; Wang, K.; Tang, Q.; Nzeukou, A.N.; Billong, N.; Melo, U.C.; Cui, X. Review on the use of volcanic ashes for engineering applications. *Resour. Conserv. Recycl.* **2018**, *137*, 177–190. [CrossRef]
44. Cheng, Y.; Wang, S.; Li, J.; Huang, X.; Li, C.; Wu, J. Engineering and mineralogical properties of stabilized expansive soil compositing lime and natural pozzolans. *Constr. Build. Mater.* **2018**, *187*, 1031–1038. [CrossRef]
45. Yin, Z.; Lekalpure, R.L.; Ndiema, K.M. Experimental Study of Black Cotton Soil Stabilization with Natural Lime and Pozzolans in Pavement Subgrade Construction. *Coatings* **2022**, *12*, 103. [CrossRef]
46. Hatefi, M.H.; Arabani, M.; Payan, M.; Zanganeh Ranjbar, P. The influence of volcanic ash (VA) on the mechanical properties and freeze-thaw durability of lime kiln dust (LKD)-stabilized kaolin clayey soil. *Results Eng.* **2024**, *24*, 103077. [CrossRef]
47. Çimen, Ö.; Keskin, N.; Kalay, E. Experimental Study to Clay Stabilization Using Waste Pumice, Waste Marble Dust and Lime. *EL-Cezeri J. Sci. Eng.* **2024**, *11*, 317–326. [CrossRef]
48. Ponce, R.; Melentijević, S.; Montero, N.; López-Andrés, S. Experimental Study on Marly Clay Stabilization Under Short-Term Conditions Using Volcanic Ash and Reactivity-Controlled Lime as Activator. *Infrastructures* **2025**, *10*, 340. [CrossRef]
49. Melentijević, S.; López Marcos, A.; Ponce, R.; López-Andrés, S. Stabilization of Expansive Clay Using Volcanic Ash. *Geosciences* **2025**, *15*, 261. [CrossRef]
50. Aqra, D.; Angin, Z.; Çelik, S.; Ikizler, S.B. Effects of using pumice, lime and marble in stabilization of expansive soils. *Rev. Constr.* **2025**, *24*, 140–151. [CrossRef]
51. Guidobaldi, G.; Cambi, C.; Cecconi, M.; Deneele, D.; Paris, M.; Russo, G.; Vitale, E. Multi-scale analysis of the mechanical improvement induced by lime addition on a pyroclastic soil. *Eng. Geol.* **2017**, *221*, 193–201. [CrossRef]
52. Aygun, Z.; Aygun, M. Spectroscopic analysis of Ahlat stone (ignimbrite) and pumice formed by volcanic activity. *Spectrochim. Acta Part A Mol. Biomol. Spectrosc.* **2016**, *166*, 73–78. [CrossRef] [PubMed]
53. Toprak, S.M.U.; Polat, R.; Levet, A.; Toprak, Ş.N. Effect of stone color, dosage and alkali type on Ahlat Stone (volcanic origin) based geopolymer concretes. *J. Build. Eng.* **2023**, *67*, 106059. [CrossRef]
54. Valido, J.A.; Cáceres, J.M.; Sousa, L.M.O. Physical and mechanical properties of Ignimbrite from Arucas, Canary Islands. *Environ. Earth Sci.* **2023**, *82*, 342. [CrossRef]
55. Morais, A.Í.; Palmeira, D.K.; Nascimento, A.M.; Osajima, J.A.; Garcia, R.R.; Huamán-Mamani, F.A. Development of Geopolymeric Mortar from Metakaolin and Ignimbrite from the Añashuayco Quarries, Peru, for Civil Construction. *Sustainability* **2025**, *17*, 5714. [CrossRef]
56. Guidobaldi, G.; Cambi, C.; Cecconi, M.; Comodi, P.; Deneele, D.; Paris, M.; Russo, G.; Vitale, E.; Zucchini, A. Chemo-mineralogical evolution and microstructural modifications of a lime treated pyroclastic soil. *Eng. Geol.* **2018**, *245*, 333–343. [CrossRef]
57. Ramos, C.G.; Querol, X.; Dalmora, A.C.; de Jesus Pires, K.C.; Schneider, I.A.H.; Oliveira, L.F.S.; Kautzmann, R.M. Evaluation of the potential of volcanic rock waste from southern Brazil as a natural soil fertilizer. *J. Clean. Prod.* **2017**, *142*, 2700–2706. [CrossRef]
58. Abousnina, R.; Aljuaydi, F.; Siddique, R.; Chen, W. Volcanic basalt quarry dust as a sustainable precursor for low-carbon geopolymer concrete. *J. Sustain. Cem.-Based Mater.* **2026**, *15*, 2347–2359. [CrossRef]
59. Akbulut, Z.F. Investigation of the change in physical, mechanical, and microstructural properties of Ahlat ignimbrites under the effect of environment and freeze-thawing. *Arab. J. Geosci.* **2022**, *15*, 472. [CrossRef]
60. Akin, M.; Topal, T.; Dinçer, İ.; Akin, M.K.; Özvan, A.; Orhan, A.; Orhan, A. A new quantitative welding degree classification for ignimbrites. *Environ. Earth Sci.* **2023**, *82*, 345. [CrossRef]
61. *ASTM D854*; Standard Test Methods for Specific Gravity of Soil Solids by Water Pycnometer. ASTM International: West Conshohocken, PA, USA, 2014.
62. *ASTM D4318-17*; Standard Test Methods for Liquid Limit, Plastic Limit, and Plasticity Index of Soils. American Society for Testing and Materials International: West Conshohocken, PA, USA, 2017.
63. *ASTM D2487-17e1*; Standard Practice for Classification of Soils for Engineering Purposes (Unified Soil Classification System). ASTM International: West Conshohocken, PA, USA, 2017.
64. *ASTM D698-12*; Standard Test Methods for Laboratory Compaction Characteristics of Soil Using Standard Effort. ASTM International: West Conshohocken, PA, USA, 2007.
65. *ASTM C204*; Standard Test Methods for Fineness of Hydraulic Cement by Air-Permeability Apparatus. American Society for Testing and Materials (ASTM): West Conshohocken, PA, USA, 2016.
66. *TS 25/T1*; Natural Pozzolan (Trass) for Use in Cement and Concrete—Definitions, Requirements and Conformity Criteria. Turkish Standards Institution: Ankara, Türkiye, 2011.
67. Ercioglu-Akdogan, N. Valorization of Ahlat Stone Wastes in the Production of Ceramic Tiles: Physical-Mechanical Properties. *Trans. Indian Ceram. Soc.* **2022**, *81*, 141–148. [CrossRef]
68. *ASTM C311/C311M-18*; Standard Test Methods for Sampling and Testing Fly Ash or Natural Pozzolans for Use in Portland-Cement Concrete. ASTM International: West Conshohocken, PA, USA, 2018.

69. Eades, J.L.; Grim, R.E. A quick test to determine lime requirements for lime stabilization. *Highw. Res. Rec.* **1966**, *139*, 61–72.
70. *ASTM D6276*; Standard Test Method for Using pH to Estimate the Soil-Lime Proportion Requirement for Soil Stabilization. ASTM International: West Conshohocken, PA, USA, 2019.
71. Zhang, J.; Li, H.; Peng, J.; Zhang, Z. Effects of Lime Content on Road Performance of Low Liquid Limit Clay. *Appl. Sci.* **2023**, *13*, 8377. [CrossRef]
72. Bilgen, G. Long-term compressive strength and microstructural appraisal of seawater, lime, and waste glass powder–treated clay soils. *Arab. J. Geosci.* **2022**, *15*, 895. [CrossRef]
73. Ahmadullah, T.; Chrysochoou, M. Relationship between strength development and pozzolanic reactions in lime stabilized kaolinite. *Int. J. Geo-Eng.* **2024**, *15*, 11. [CrossRef]
74. Babanas, H.; Courcelles, B. Enhancing Lime Dosage Determination for Lean Clay Soil Improvement: Significance of Plasticity Limit and Interpretation Approach. *Geotechnics* **2025**, *5*, 9. [CrossRef]
75. Naveed, M.A.; Ahmed, S.; Ullah, A.; Zia, M.D. Mechanism of improvement and best-fit models for the prediction of geotechnical properties of lime stabilized expansive soil used in pavement subgrade. *Mehran Univ. Res. J. Eng. Technol.* **2024**, *43*, 65–78. [CrossRef]
76. Sendilvadivelu, A.; Dhandapani, B.; Vijayasimhan, S.; Pauldurai Kalaiselvi, S.P. Sustainable Stabilization of Clay Soil Using Lime and *Oryza sativa*-Waste-Derived Dried Solid Digestate. *Sustainability* **2025**, *17*, 8447. [CrossRef]
77. Cherian, C.; Arnepalli, D.N. A Critical Appraisal of the Role of Clay Mineralogy in Lime Stabilization. *Int. J. Geosynth. Ground Eng.* **2015**, *1*, 8. [CrossRef]
78. Jiang, Y.; Ying, Z.; Liu, F.; Jiang, C.; Wang, S.; Deng, Y. Long-term performance of lime-treated soil and chemical reaction identification. *J. Rock Mech. Geotech. Eng.* **2025**, *17*, 5146–5154. [CrossRef]
79. Fode, T.A.; Jande, Y.A.C.; Kivevele, T. Effect of Natural Pozzolana on Physical and Mechanical Properties of Concrete. *Adv. Civ. Eng.* **2024**, *2024*, 3356641. [CrossRef]
80. *ASTM D2166/D2166M-16*; Standard Test Method for Unconfined Compressive Strength of Cohesive Soil. American Society for Testing and Materials (ASTM): West Conshohocken, PA, USA, 2016.
81. *ASTM D1883*; Standard Test Method for California Bearing Ratio (CBR) of Laboratory-Compacted Soils. ASTM International: West Conshohocken, PA, USA, 2021.
82. Harichane, K.; Ghrici, M.; Gadouri, H. Natural pozzolana used as a source of silica for improving the behaviour of lime–stabilised clayey soil. *Arab. J. Geosci.* **2019**, *12*, 447. [CrossRef]
83. Driss, A.A.E.; Harichane, K.; Ghrici, M.; Mohammed, A.S. Enhancing Geotechnical Properties of Expansive Clay with Lime and Natural Pozzolana: Experimental and Microstructural Analysis. *Arab. J. Sci. Eng.* **2025**, *50*, 16933–16955. [CrossRef]
84. Harichane, K.; Ghrici, M.; Kenai, S.; Grine, K. Use of Natural Pozzolana and Lime for Stabilization of Cohesive Soils. *Geotech. Geol. Eng.* **2011**, *29*, 759–769. [CrossRef]
85. Estabragh, A.R.; Jahani, A.; Javadi, A.A.; Babalar, M. Assessment of different agents for stabilisation of a clay soil. *Int. J. Pavement Eng.* **2022**, *23*, 160–170. [CrossRef]
86. Moayed, S.A.M.; Arabani, M.; Ahmadi, H. Influence of hemp fiber on the mechanical characteristics and freeze-thaw durability of LKD-nano silica-stabilized kaolin soil. *Results Eng.* **2025**, *26*, 105318. [CrossRef]
87. Borges, A.L.; Laura, S.A.A.; Freitas, T.O.G.; Ferreira, F.G.d.S. Filler effect and pozzolanic effect of glass powder in mortar. *Ambient. Constr.* **2025**, *25*, e144814. [CrossRef]
88. Noaman, M.A.; Karim, M.R.; Islam, M.N. Comparative study of pozzolanic and filler effect of rice husk ash on the mechanical properties and microstructure of brick aggregate concrete. *Heliyon* **2019**, *5*, e01926. [CrossRef] [PubMed]
89. Kaminskas, R.; Barauskas, I.; Kubiliute, R.; Monstvilaite, D. The effect of the pozzolanic activity of different micro-fillers on Portland cement hydration. *Ceramics-Silikaty* **2020**, *64*, 145–154. [CrossRef]
90. Rabab'ah, S.R.; Sharo, A.A.; Alqudah, M.M.; Ashteyat, A.M.; Saleh, H.O. Effect of using Oil Shale Ash on geotechnical properties of cement-stabilized expansive soil for pavement applications. *Case Stud. Constr. Mater.* **2023**, *19*, e02508. [CrossRef]
91. Preetham, H.K.; Nayak, S. Geotechnical Investigations on Marine Clay Stabilized Using Granulated Blast Furnace Slag and Cement. *Int. J. Geosynth. Ground Eng.* **2019**, *5*, 28. [CrossRef]
92. Saeed, K.; Kassim, K.; Yunus, N.; Nur, H. Characterization of hydrated lime-stabilized brown kaolin clay. *Int. J. Eng. Res. Technol.* **2013**, *2*, 3722–3727. [CrossRef]
93. Wong, J.K.H.; Kok, S.T.; Wong, S.Y. Cementitious, pozzolanic and filler materials for DSM binders. *Civ. Eng. J.* **2020**, *6*, 402–417. [CrossRef]
94. Salimi, M.; Dordsheykhtorkamani, A.; Afrasiabian, A.; Khajeh, A. Incorporation of Volcanic Ash for Enhanced Treatment of a Cement-Stabilized Clayey Soil. *J. Mater. Civ. Eng.* **2021**, *33*, 04020465. [CrossRef]
95. L'Hôpital, E.; Lothenbach, B.; Le Saout, G.; Kulik, D.; Scrivener, K. Incorporation of aluminium in calcium-silicate-hydrates. *Cem. Concr. Res.* **2015**, *75*, 91–103. [CrossRef]

96. Hatefi, M.H.; Arabani, M.; Payan, M.; Ranjbar, P.Z. Impact of recycled macro-synthetic fibers on kaolin soil stabilized with lime kiln dust and volcanic ash. *Case Stud. Constr. Mater.* **2025**, *22*, e04830. [CrossRef]
97. Mousavi, S.E. Utilization of Silica Fume to Maximize the Filler and Pozzolanic Effects of Stabilized Soil with Cement. *Geotech. Geol. Eng.* **2018**, *36*, 77–87. [CrossRef]
98. Bahmyari, H.; Ajdari, M.; Vakili, A.; Ahmadi, M.H. The Role of the Cement, Lime, and Natural Pozzolan Stabilizations on the Mechanical Response of a Collapsible Soil. *Transp. Infrastruct. Geotechnol.* **2021**, *8*, 452–472. [CrossRef]
99. Wang, Y.Z.; Chen, F.Y.; Gao, Y.; Zhuang, M.L.; Ge, F.H.; Tang, Z.J. Unconfined Compressive Strength Optimization of Industrial Solid Waste-Based Soil Stabilizers. *Strength Mater.* **2025**, *57*, 1357–1364. [CrossRef]
100. Soltani, A.; Aminaee, A.; Abed, P. Improving Mechanical Properties of Low-Strength Kaolin Clay by Mixing Nano Hydro Carbonated Shale and Quicklime. *Int. J. Geosynth. Ground Eng.* **2024**, *10*, 53. [CrossRef]
101. Aksu Alcan, B.; Kara, H.O.; Yılmazoğlu, M.U. Geopolymerization of Kaolin Clay with Hemp Fibers for Sustainable Soil Stabilization. *Polymers* **2025**, *17*, 3216. [CrossRef] [PubMed]
102. Basha, E.A.; Hashim, R.; Mahmud, H.B.; Muntohar, A.S. Stabilization of residual soil with rice husk ash and cement. *Constr. Build. Mater.* **2005**, *19*, 448–453. [CrossRef]
103. Sharma, N.K.; Swain, S.K.; Sahoo, U.C. Stabilization of a Clayey Soil with Fly Ash and Lime: A Micro Level Investigation. *Geotech. Geol. Eng.* **2012**, *30*, 1197–1205. [CrossRef]
104. Mishra, E.N.K. Strength Characteristics of Clayey Sub-Grade Soil Stabilized with Fly Ash and Lime for Road Works. *Indian Geotech. J.* **2012**, *42*, 206–211. [CrossRef]
105. Al-Swaidani, A.M.; Meziab, A.; Khwies, W.T.; Al-Bali, M.; Lala, T. Building MLR, ANN and FL models to predict the strength of problematic clayey soil stabilized with a combination of nano lime and nano pozzolan of natural sources for pavement construction. *Int. J. Geo-Eng.* **2024**, *15*, 2. [CrossRef]
106. Yu, B.; Ma, Q.; Liu, S.; Hu, X.; Sun, C.; Jiang, N. Utilization of calcium carbide residue based soil stabilizer in road construction: Strength, environmental impact, and field application. *Transp. Geotech.* **2024**, *49*, 101422. [CrossRef]
107. Özvan, A.; Dinçer, İ.; Akın, M.; Oyan, V.; Tapan, M. Experimental studies on ignimbrite and the effect of lichens and capillarity on the deterioration of Seljuk Gravestones. *Eng. Geol.* **2015**, *185*, 81–95. [CrossRef]
108. Alraddadi, S. Effects of calcination on structural properties and surface morphology of black volcanic ash. *J. Phys. Commun.* **2020**, *4*, 105002. [CrossRef]
109. Henderson, M.J.B.; Horgan, B.H.N.; Rowe, M.C.; Wall, K.T.; Scudder, N.A. Determining the Volcanic Eruption Style of Tephra Deposits from Infrared Spectroscopy. *Earth Space Sci.* **2021**, *8*, e2019EA001013. [CrossRef]
110. Akula, P.; Little, D.N. Analytical tests to evaluate pozzolanic reaction in lime stabilized soils. *MethodsX* **2020**, *7*, 100928. [CrossRef]
111. Firat, S.; Khatib, J.M.; Yilmaz, G.; Comert, A. Effect of curing time on selected properties of soil stabilized with fly ash, marble dust and waste sand for road sub-base materials. *Waste Manag. Res.* **2017**, *35*, 747–756. [CrossRef] [PubMed]
112. Yusuf, M.O. Bond Characterization in Cementitious Material Binders Using Fourier-Transform Infrared Spectroscopy. *Appl. Sci.* **2023**, *13*, 3353. [CrossRef]
113. Fernández, L.J. Infrared Spectroscopy in the Analysis of Building and Construction Materials. In *Infrared Spectroscopy—Materials Science, Engineering and Technology*; Theophanides, T., Ed.; IntechOpen: London, UK, 2012.
114. Kloprogge, J.T. *Spectroscopic Methods in the Study of Kaolin Minerals and Their Modifications*; Springer: Berlin/Heidelberg, Germany, 2019.
115. Abo-El-Enein, S.A.; Heikal, M.; Amin, M.S.; Negm, H.H. Reactivity of dealuminated kaolin and burnt kaolin using cement kiln dust or hydrated lime as activators. *Constr. Build. Mater.* **2013**, *47*, 1451–1460. [CrossRef]
116. Vilasini, P.; Thangasamy, L.; Balu, S. Analysis on the lime stabilization of pond ash for enhanced strength and environmental impact reduction. *Constr. Build. Mater.* **2025**, *490*, 142590. [CrossRef]
117. Majd Rahimabadi, M.; Arabani, M. Impact of lime kiln dust on the mechanical properties and freeze-thaw durability of nanoclay-stabilized kaolin soil. *Case Stud. Constr. Mater.* **2026**, *24*, e05774. [CrossRef]
118. Gupta, S.; Kumar, S. Mechanical and microstructural analysis of soft kaolin clay stabilized by GGBS and dolomite-based geopolymer. *Constr. Build. Mater.* **2024**, *421*, 135702. [CrossRef]
119. Kumar, A.; Lingfa, P. Sodium bentonite and kaolin clays: Comparative study on their FT-IR, XRF, and XRD. *Mater. Today Proc.* **2020**, *22*, 737–742. [CrossRef]
120. Saeed, K.A.H.; Kassim, K.A.; Yunus, N.M.; Nur, H.; Abdul Hussein Saeed, K.; Kassim, K.; Mohd Yunus, N.; Nur, H. Physico-chemical characterization of lime stabilized tropical kaolin clay. *J. Teknol.* **2015**, *72*, 83–90. [CrossRef]
121. Prabawa, I.D.G.P.; Lestari, R.Y.; Hamdi, S.; Sunardi. Modified physical properties of kaolin by intercalation and exfoliation method. In *IOP Conference Series: Materials Science and Engineering*; IOP Publishing: Bristol, UK, 2020; Volume 980, p. 012009. [CrossRef]
122. Li, Q.; Li, Q.; Wang, F.; Xu, N.; Wang, Y.; Bai, B. Settling behavior and mechanism analysis of kaolinite as a fracture proppant of hydrocarbon reservoirs in CO_2 fracturing fluid. *Colloids Surf. A Physicochem. Eng. Asp.* **2025**, *724*, 137463. [CrossRef]

123. Li, Q.; Li, Q.; Wang, F.; Wu, J.; Wang, Y.; Jin, J. Effects of Geological and Fluid Characteristics on the Injection Filtration of Hydraulic Fracturing Fluid in the Wellbores of Shale Reservoirs: Numerical Analysis and Mechanism Determination. *Processes* **2025**, *13*, 1747. [CrossRef]
124. Soltaninejad, S.; Marandi, S.M.; B.P., N. Effects of the Types and Amounts of Clay Minerals on Durability of Lime-Stabilized Clay Soils. *Minerals* **2023**, *13*, 1317. [CrossRef]
125. Pérez-Arévalo, S.; Millán-Franco, M.A.; Aguilar-Reyes, B.O.; Reyes-Gasga, J. Structural and chemical characterization of kaolinite from the Capula clay in Michoacán region, Mexico, by X-ray diffraction and electron microscopy. *Ceram. Int.* **2025**, *51*, 55020–55029. [CrossRef]
126. Wilkinson, A.; Haque, A.; Kodikara, J. Stabilisation of clayey soils with industrial by-products: Part A. *Proc. Inst. Civ. Eng.-Ground Improv.* **2010**, *163*, 149–163. [CrossRef]
127. Avşar, E.; Işık, E. Environmental toxicity characteristics of Nemrut volcanism pyroclastic, Bitlis/Turkey case. *Sigma J. Eng. Nat. Sci.* **2020**, *38*, 1203–1215.

Disclaimer/Publisher's Note: The statements, opinions and data contained in all publications are solely those of the individual author(s) and contributor(s) and not of MDPI and/or the editor(s). MDPI and/or the editor(s) disclaim responsibility for any injury to people or property resulting from any ideas, methods, instructions or products referred to in the content.